Errata

Document Title: Microwave Power Generation and Amplification Using IMPATT Diodes (AN 935)

Part Number: 5952-0260

Revision Date: June 1971

HP References in this Application Note

This application note may contain references to HP or Hewlett-Packard. Please note that Hewlett-Packard's former test and measurement, semiconductor products and chemical analysis businesses are now part of Agilent Technologies. We have made no changes to this application note copy. The HP XXXX referred to in this document is now the Agilent XXXX. For example, model number HP8648A is now model number Agilent 8648A.

About this Application Note

We've added this application note to the Agilent website in an effort to help you support your product. This manual provides the best information we could find. It may be incomplete or contain dated information, and the scan quality may not be ideal. If we find a better copy in the future, we will add it to the Agilent website.

Support for Your Product

Agilent no longer sells or supports this product. You will find any other available product information on the Agilent website:

www.agilent.com

Search for the model number of this product, and the resulting product page will guide you to any available information. Our service centers may be able to perform calibration if no repair parts are needed, but no other support from Agilent is available.

Agilent Technologies

APPLICATION NOTE 935

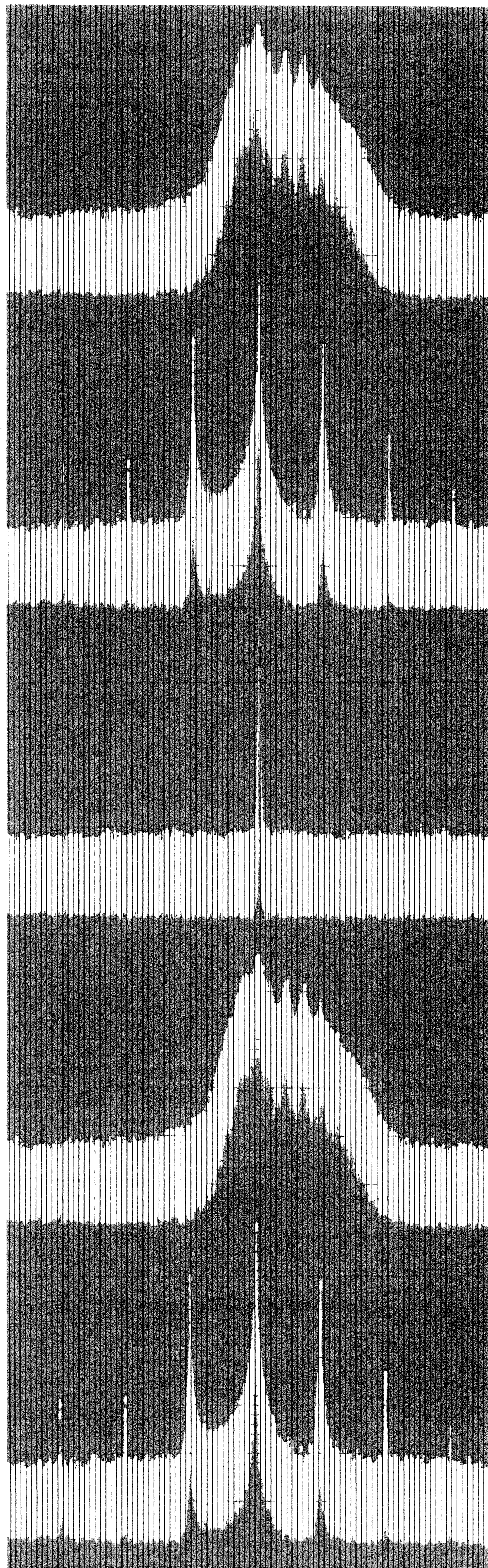

MICROWAVE POWER GENERATION AND AMPLIFICATION USING IMPATT DIODES

HEWLETT hp PACKARD

COMPONENTS

CONTENTS

Page No.

I. Introduction 1

II. Device Theory and Construction 1
- A) *Device Structure and DC Characteristics* 1
- B) *Microwave Properties* 1
- C) *Diode Construction* 3

III. General Design Considerations and Operating Precautions 4
- A) *Packaged Diode Equivalent Circuit* 4
- B) *Diode Mounting Techniques* 4
- C) *Thermal Resistance Measurement* 6
- D) *Bias Circuits* 8
- E) *Operating Precautions* 9

IV. Broadly Tunable Circuits 10
- A) *Multiple Slug Tuned Cavity; Bias T* 10
- B) *Variable Industance Tunable Coaxial Circuit* 12
- C) *Tunable Waveguide Oscillator* 14

V. Low Q Fixed-Tuned IMPATT Oscillators and Amplifiers 15
- A) *Oscillator Circuits* 17
- B) *Amplifier Circuits* 18
- C) *Power Combining Techniques* 21

VI. High Q Low Noise Oscillators 22
- A) *Coupled Coaxial-Waveguide Oscillator* 22
- B) *Low Cost Waveguide Oscillator* 24
- C) *Varactor Tuning* 24

VII. Noise in IMPATT Oscillators 25
- A) *Noise Theory* 25
- B) *Typical Data* 27
- C) *Noise Suppression* 28

APPENDIX A – IMPATT CIRCUIT DRAWINGS AVAILABLE FROM HP 30

I. Introduction

The generation of microwave power in a reverse-biased pn junction was originally suggested in 1958 by W. T. Read of Bell Telephone Laboratories[1]. Read proposed that the finite delay between an applied RF voltage and the current generated by avalanche breakdown, and the subsequent drift of the generated carriers through the depletion layer of the junction, would lead to negative resistance at microwave frequencies in a properly designed diode. This basic concept has been shown to be substantially correct, and at this time, microwave avalanche diodes (commonly called IMPATT* diodes) are commercially available and are being used in a variety of applications. The purpose of this Application Note is to acquaint the reader with the construction and the principles of operation of IMPATT diodes, and to provide practical circuit designs and operating guidelines for HP's family of IMPATT diodes.

II. Device Theory and Construction

A) *Device Structure and DC Characteristics*

The basic structure of a silicon pn junction IMPATT diode, from the semiconductor point of view, is identical to that of microwave tuning and parametric amplifier varactor diodes. The important differences between IMPATT and varactor diodes are in their modes of operation, and in thermal design.

Fig. 1 shows a typical dc current versus voltage ("VI") characteristic for a pn junction diode. In the forward bias direction, the current increases rapidly for voltages above 0.5 volts or so. In the reverse direction, a very small current (the "saturation" or "leakage" current) flows until the breakdown voltage, V_b, is reached. Varactor diodes normally operate either forward biased or reverse biased with a dc operating point well below V_b. IMPATT diodes, on the other hand, operate in the avalanche breakdown region; that is, with a dc reverse voltage greater than V_b and substantial reverse current flowing.

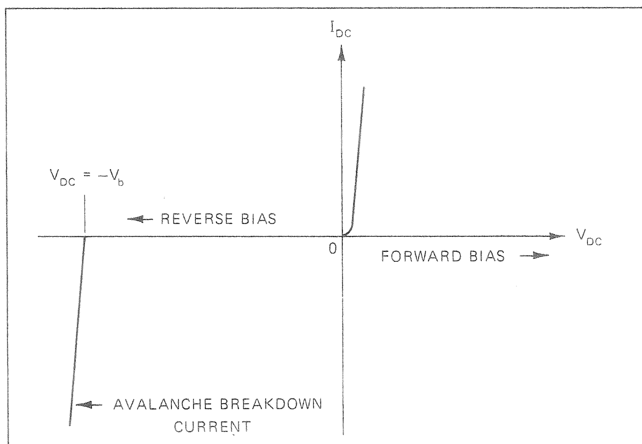

Fig. 1 Terminal V–I Characteristics of a PN Junction Diode.

*This word is an acronym suggested by scientists at Bell Telephone Laboratories: It stands for IMPact ionization Avalanche Transit Time.

Fig. 2 shows a schematic representation of an IMPATT diode reverse biased into avalanche breakdown. As in any reverse biased pn junction, a *depletion zone* forms in the n-type region of the diode; its width depends on the applied reverse voltage. The depletion zone acts as a nonlinear capacitor if V_{BAT} is less than V_b; this property is utilized in varactor diodes. The saturation current, which flows while the reverse voltage is less than V_b, is usually on the order of 10 to 100 nanoamperes, and is depicted in Fig. 2 by a small number of electrons flowing to the right from the P^+ region into the *avalanche zone*. When V_{BAT} is greater than V_b, the small number of electrons comprising the saturation current have a very high probability of creating additional electrons and holes in the avalanche zone by the process of avalanche multiplication. The additional electrons are shown in Fig. 2 flowing from the avalanche zone into the *drift zone*. In this condition, a large current can flow in the reverse direction with little increase in applied voltage. This is the *avalanche breakdown current* depicted in Fig. 1. The typical dc operating voltage across a diode designed for use in X-band will be between 70 and 100 volts, depending on the diode type, temperature, and the value of the bias current, I_{DC}. Typical avalanche breakdown currents (usually called the "bias current", and denoted in this Application Note by I_{DC}) range from 20 to 150 mA.

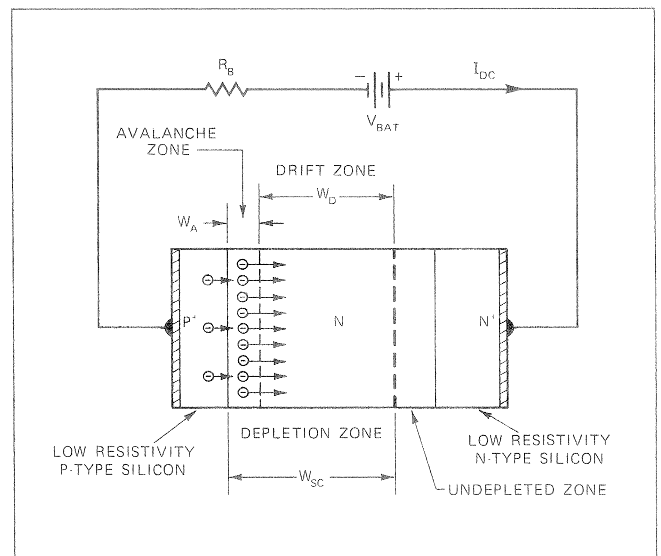

Fig. 2 Schematic Representation of Reverse-Biased PN Junction Diode.

B) *Microwave Properties*

The microwave properties of IMPATT diodes have been described extensively in the literature; references [1], [2] and [3] explain quite clearly the basic concepts involved. We will briefly discuss the major points in the derivation of microwave *negative resistance* in the following paragraphs.

Let us assume that somehow an RF voltage, in addition to the DC breakdown voltage, exists across the depletion region of the IMPATT diode. This voltage can be expressed mathematically as

$$V_T(t) = V_{DC} + V_D \sin \omega t \quad (1)$$

This form of voltage is illustrated in Fig. 3A and would exist in practice in the common case where the diode is operated in a singly resonant circuit with Q greater than 10 or so. Read[1] showed that under certain conditions the RF portion of this voltage induces an RF current that is more than 90° out of phase with the voltage, and that therefore the diode has negative resistance. The arguments leading to this conclusion are conveniently divided into two steps:

First, Read showed that as the voltage rises above the DC breakdown voltage during the positive half cycle of the RF voltage, excess charge builds up in the avalanche region slowly at first, and reaches a sharply-peaked maximum at $\omega t \approx \pi$, that is, in the middle of the RF voltage cycle when the RF voltage is zero. This is shown in Fig. 3B. Thus the charge generation waveform, in addition to being very sharply peaked, *lags* the RF voltage by 90°. This behavior arises because of the highly nonlinear nature of the avalanche generation process.

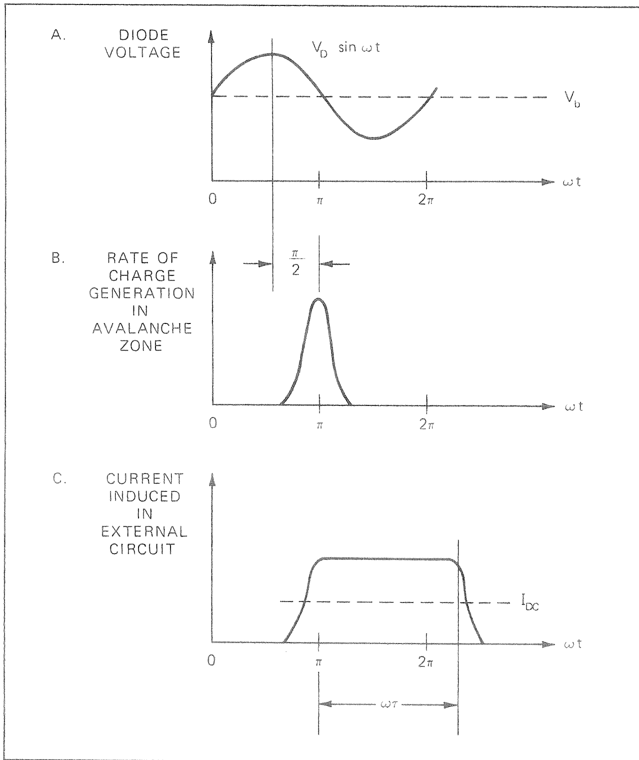

Fig. 3A. Voltage Across the IMPATT Diode Depletion Layer During Oscillation.
Fig. 3B. Rate of Charge Generation in the Avalanche Zone.
Fig. 3C. Current Induced in the External Circuit by the Avalanche Generated Charge Drifting Across the Drift Zone.

The second step in the analysis was to consider the behavior of the generated charge subsequent to $\omega t = \pi$. The direction of the field is such that, referring to Fig. 2, the electrons "drift" to the right. The equal number of generated holes move to the left, back into the P^+ contact, and are not considered further in this simple model. The electrons drift at constant ("saturated") velocity, v_{sat}, across the drift zone. The time, τ, they take to traverse the drift zone is simply the width of the drift zone divided by the constant velocity of the electrons:

$$\tau = \frac{W_D}{v_{sat}} \quad (2)$$

While the electrons are drifting through the diode, they induce a current in the external circuit, as shown in Fig. 3C. The current is approximately a square wave. By examining Figs. 3A and 3C, it can now be seen that the combined delay of the avalanche process and the finite transit time across the drift zone have caused *positive* current to flow in the external circuit while the diode's RF voltage is going through its *negative* half cycle. The diode is thus delivering RF energy to the external circuit, or in circuit terms, is exhibiting *negative resistance*. Maximum negative resistance is obtained when

$$\omega\tau \simeq 0.74\,\pi \quad (3)$$

The term $\omega\tau$ is called the *transit angle*; IMPATT diodes are normally designed so that Eq. (3) is satisfied at or near the center of the desired operating frequency range.

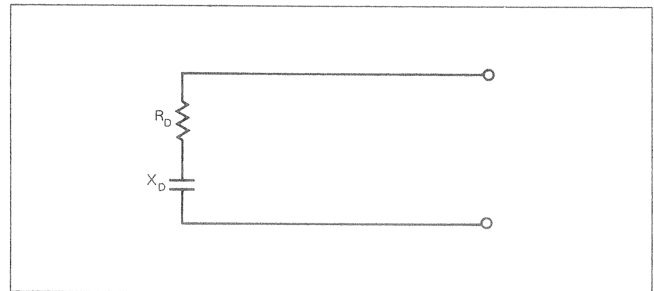

Fig. 4. IMPATT Diode Chip RF Equivalent Circuit.

An equivalent circuit for the IMPATT diode chip is shown in Fig. 4. Here we show the active part of the diode (the chip, excluding the package) as a negative resistance R_D, and a reactance X_D. Included in R_D is the unavoidable parasitic series resistance, R_s, contributed by the contacts and the undepleted portion of the N region shown in Fig. 2. Several important properties of the IMPATT diode chip equivalent circuit deserve comment. *First*, the magnitude of the net negative resistance R_D, is usually much smaller than that of X_D, the reactance. Consequently, the magnitude of the chip impedance is approximately X_D. *Second*, for most cases of interest, X_D can be approximated with sufficient accuracy by the reactance of the junction (chip) capacitance at the breakdown voltage. This capacitance is denoted by $C_j(V_b)$; typical values of $C_j(V_b)$ for HP IMPATT diodes are given in Table I on page 4. *Third*, values of the net negative resistance are generally small compared to the usual transmission line impedances. Typical values are in the vicinity of several ohms; Table I lists measured values for HP IMPATT diodes. The *fourth* and final point regards the behavior of the IMPATT diode negative resistance with signal level: As in *any* active oscillator element, the IMPATT negative resistance varies with signal level. A typical example

is shown in Fig. 5, where the magnitude of R_D (R_D is a negative number) is shown plotted versus peak RF diode current, I_D. The decrease of $|R_D|$ with signal level is what leads to stable oscillations. It might also be remarked at this point that R_D varies with bias current as well as with signal level. Complete curves of R_D vs. I_D with bias current as a parameter are presented in Section V, part B.

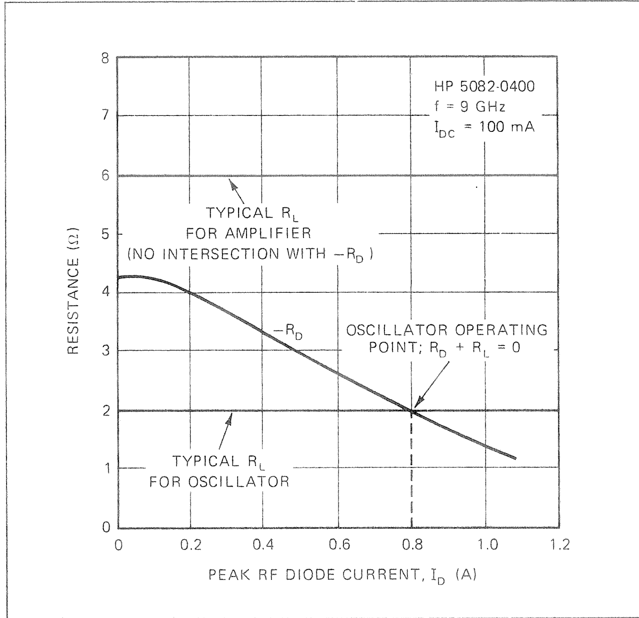

Fig. 5. Variation of R_D (a Negative Number) with RF Current Amplitude I_D. The Operating Point is Determined by the Condition $R_L = -R_D$.

We have now shown qualitatively how negative resistance arises in an IMPATT diode, and have given a quantitative example of how it varies with signal level — the next step is to consider how the IMPATT chip interacts with an external circuit: Basic oscillator theory states that oscillation will occur if, at some frequency, the load impedance connected to the IMPATT chip is the *negative* of the chip impedance. (See Fig. 6). Since the chip is *capacitive*; the load must be inductive; the real part of the load resistance must be in the range of several ohms, and more specifically, must be *less* than the maximum value of $|R_D|$. If these conditions are satisfied, oscillations will build up in the circuit at the frequency for which $X_D = -X_L$. The oscillations will continue to build up until $R_L + R_D = 0$; this is a stable "operating point", and is shown in Fig. 5. In actual circuits to be considered in subsequent sections, we will find that most or all of the required load inductance will be provided by the IMPATT diode package itself; the package equivalent circuit is discussed in Section III.

The power delivered to the load by the IMPATT diode can be calculated from the operating point coordinates (R_L, I_D) using the relation

$$P_o = \tfrac{1}{2} I_D^2 R_L \quad (4)$$

For the example shown in Fig. 5, we have I_D = 0.80A, R_L = 2.0 Ω, and we find P_o from (4) to be 0.64 W.

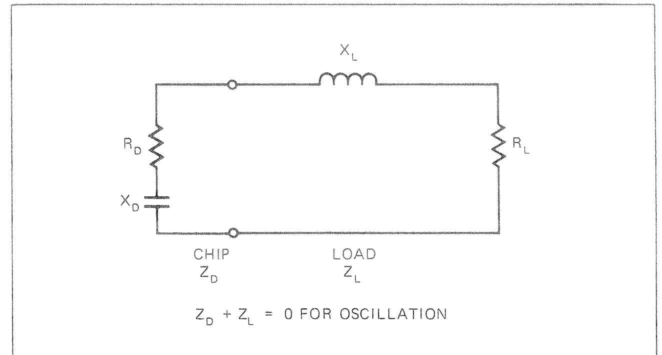

Fig. 6. Equivalent Circuit for the IMPATT Diode Chip, Showing the Form of a Typical Load Impedance.

Fig. 5 also shows a curve for R_L = 6 Ω, which does not intersect the $|R_D|$ vs. I_D curve. No oscillation is possible in this circumstance, but the circuit can behave as a reflection amplifier if a means of separating input and output signals, such as a circulator, is provided. Amplifiers are an important application for IMPATT diodes, and are discussed more fully in Section V.

C) *Diode Construction*

The construction of IMPATT diodes poses some severe technological challenges, the most troublesome one being the efficient extraction of heat from the active portion of the diode. Hewlett-Packard has developed a unique technique for reducing junction heating by using an electroplating process to form the critical portion of the heat sink — that nearest the pn junction. The chip which results from the Hewlett-Packard process is shown in Fig. 7. Fig. 8 shows in cross-section the chip soldered into the HP Style 41 metal-ceramic microwave package. The thermal resistance obtained by this process is close to the theoretical ideal, and is very reproducible, resulting in high yields. The assembly process is also faster than the conventional process which, combined with the high yield, represents a considerable economy in overall fabrication cost. Hewlett-Packard IMPATT diodes, the 5082-0430 series in particular, are accordingly very attractive for price-sensitive applications such as low-cost intrusion alarms, educational laboratory demonstrations, and fuses.

The reader who is interested in further details of the fabrication of HP IMPATT diodes is referred to References [4] and [5], listed at the end of this Application Note.

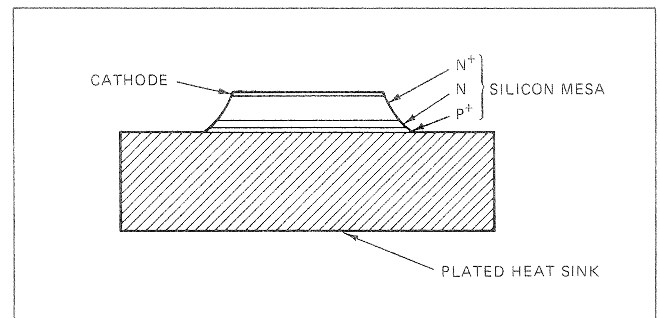

Fig. 7. HP Plated-Heat-Sink IMPATT Diode Chip.

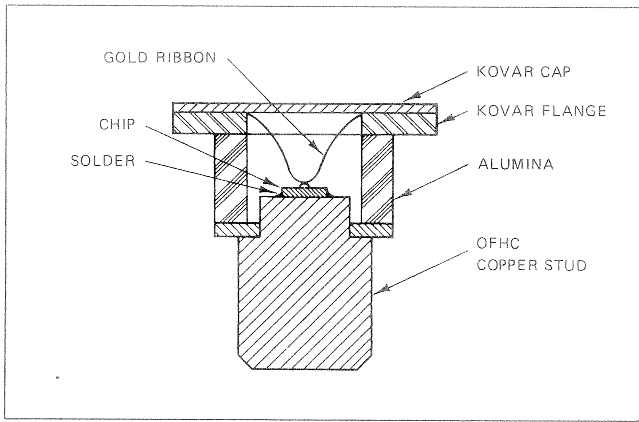

Fig. 8. Cross Section of the HP IMPATT Diode Chip in Style 41 Package.

III. General Design Considerations and Operating Precautions

A) *Packaged Diode Equivalent Circuit*

The diode chip equivalent circuit is considerably modified by the presence of the varactor package parasitic reactances. Up to now we have been discussing the properties of the chip by itself, but in microwave circuit design the entire packaged diode must be considered. To a good approximation, the package can be described by two reactive elements, a series inductance and a shunt capacitance. The complete packaged IMPATT diode equivalent circuit is shown in Fig. 9A. The exact values of L_p and C_p vary somewhat from one package style to another, but typical values (for the HP Style 41 package end-mounted in 7 mm coax, as an example) are 0.6 nh and 0.3 pf, respectively. The value of L_p is affected drastically by the microwave circuit surrounding the diode — this fact can be used to tune an oscillator, and is described in Section IV.B.

Typical values of the circuit elements for the HP 5082-0400 diode are shown in Fig. 9B; the value of R_D corresponds to an output power of about 700 mW as an oscillator. We notice that the IMPATT package inductance

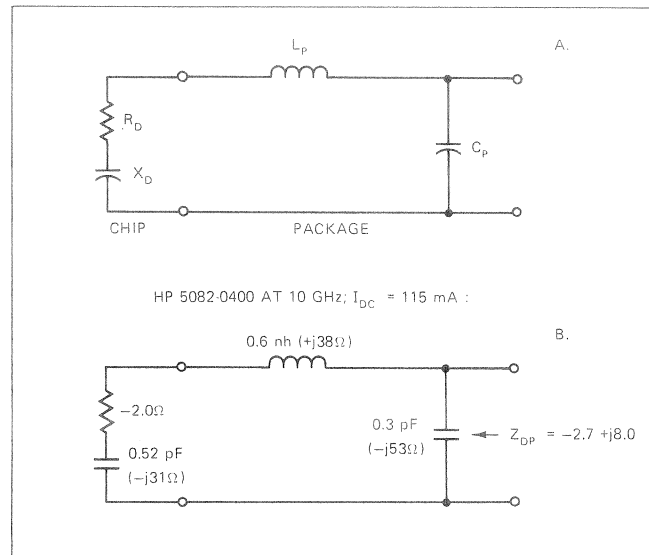

Fig. 9A. Equivalent Circuit of the Packaged IMPATT Diode Showing Package Parasitics.

Fig. 9B. Typical Values of the HP 5082-0400 IMPATT Diode Circuit Elements at 10 GHz with I_{DC} = 115 mA.

very nearly resonates the chip capacitance, $C_j(V_b)$, so that the reactance presented by the chip at the package terminals is relatively small. The overall impedance of the packaged diode is shown for this case as $Z_{DP} = -2.7 + j8.0\ \Omega$.

Table I shows typical values of HP IMPATT diode equivalent circuit parameters at specific test frequencies. Note that the value for R_D, the negative resistance, is that corresponding to the output power listed in the P_o column; it is always important to state the rf signal level in some way when specifying R_D, since as discussed in Section II.B, R_D is a strong function of signal level. The bias currents at which the listed values of R_D and P_o are obtained are listed in the last column.

B) *Diode Mounting Techniques*

There are a number of ways to mount HP IMPATT diodes in microwave circuits. General considerations in

TABLE I: Circuit Parameters for Hewlett-Packard IMPATT Diodes

DIODE TYPE 5082-	APPROX. TEST FREQ. (GHz)	C_j $V = V_b$ (pf)	R_D at P_o (typ) (Ω)	P_o (typ) (W)	R_s (typ) (Ω)	V_b (typ) (v)	C_p (typ) (pf)	L_p (typ) (nh*)	PACKAGE STYLE	I_{DC} (typ) (mA)
0400	10	0.52	−2.0	0.7	1.0	78	0.3	0.6	41	115
0401	12	0.57	−1.8	0.6	0.7	65	0.3	0.6	41	130
0431	6.5	0.29	−0.9	0.1	0.9	103	0.3	0.6	41	28
0432	10	0.20	−0.7	0.1	1.6	78	0.3	0.6	41	30
0433	12	0.31	−1.0	0.1	1.5	65	0.3	0.6	41	34
0434	6.5	0.29	−0.9	0.1	0.9	103	0.3	0.6	62	28
0435	10	0.20	−0.7	0.1	1.6	78	0.3	0.6	62	30
0436	12	0.31	−1.0	0.1	1.5	65	0.3	0.6	62	34
0437	6.5	0.29	−0.9	0.1	0.9	103	0.26	1.0	32	28
0438	10	0.20	−0.7	0.1	1.6	78	0.26	1.0	32	30
0439	12	0.31	−1.0	0.1	1.5	65	0.26	1.0	32	34

*Measured for end-mounted diode in 0.276" O.D. 50 Ω coaxial transmission line. L_p varies considerably with circuit configuration—see Sections IV and V.

mounting are that the diode be provided with a good heat flow path to a heat sink or heat dissipator held at the ambient temperature, and that low resistance electrical contacts be made to both anode and cathode of the diode.

Fig. 10 shows several mounting techniques for IMPATT diodes. The collet-clamp-sleeve arrangement of Fig. 10A is especially suitable for end-mounting diodes in coaxial circuits, and provides a convenient mount for laboratory breadborading or test fixtures, where quick interchangeability of diodes is desirable; the parts are made of Tellurium Copper or Berylco 10, both of which are readily machinable and have nearly the thermal conductivity of copper. OFHC copper can also be used, at a sacrifice of ease of machinability and resistance to wear. The diode holder assembly consists of four parts: A *diode collet* for gripping the heat sink end of the diode, a sleeve into which the diode collet is inserted, a *knurled nut* which pulls the collet tightly into the sleeve, and a *clamp*. The clamp is screwed into the cavity body, and is tightened after the sleeve containing diode and collet has been inserted and held with moderate pressure against the coaxial center conductor. This arrangement allows easy interchangeability of diodes and ensures a low electrical and thermal resistance contact between diode and cavity. For a diode package with threaded stud (HP Style 62) the collet and sleeve are replaced by a Tellerium-Copper part having the same outer dimensions as the sleeve, but with a threaded hole to accommodate the stud, and a hole down the center for insertion of a screwdriver to tighten the diode. This part is also shown in Fig. 10A, together with a *recessed* collet. Recessed collets are discussed later, in the circuit design sections.

A variation of the scheme of Fig. 10A is shown in Fig. 10B. Here the collet is screwed into the large mounting screw, which can in turn be screwed into the microwave circuit. This arrangement provides permanent, secure mounting, while offering the feature of easy diode replacement if circumstances require it. Fig. 10C shows the HP 41 package soldered into the mounting screw – diode replacement is more difficult in this case, but superior heat sinking and resistance to vibration and shock are obtained. This method is potentially cheaper, too, since fewer parts are required. The method of Fig. 10C can be adapted to Style 62 (screw stud) package by simply threading the mounting screw to

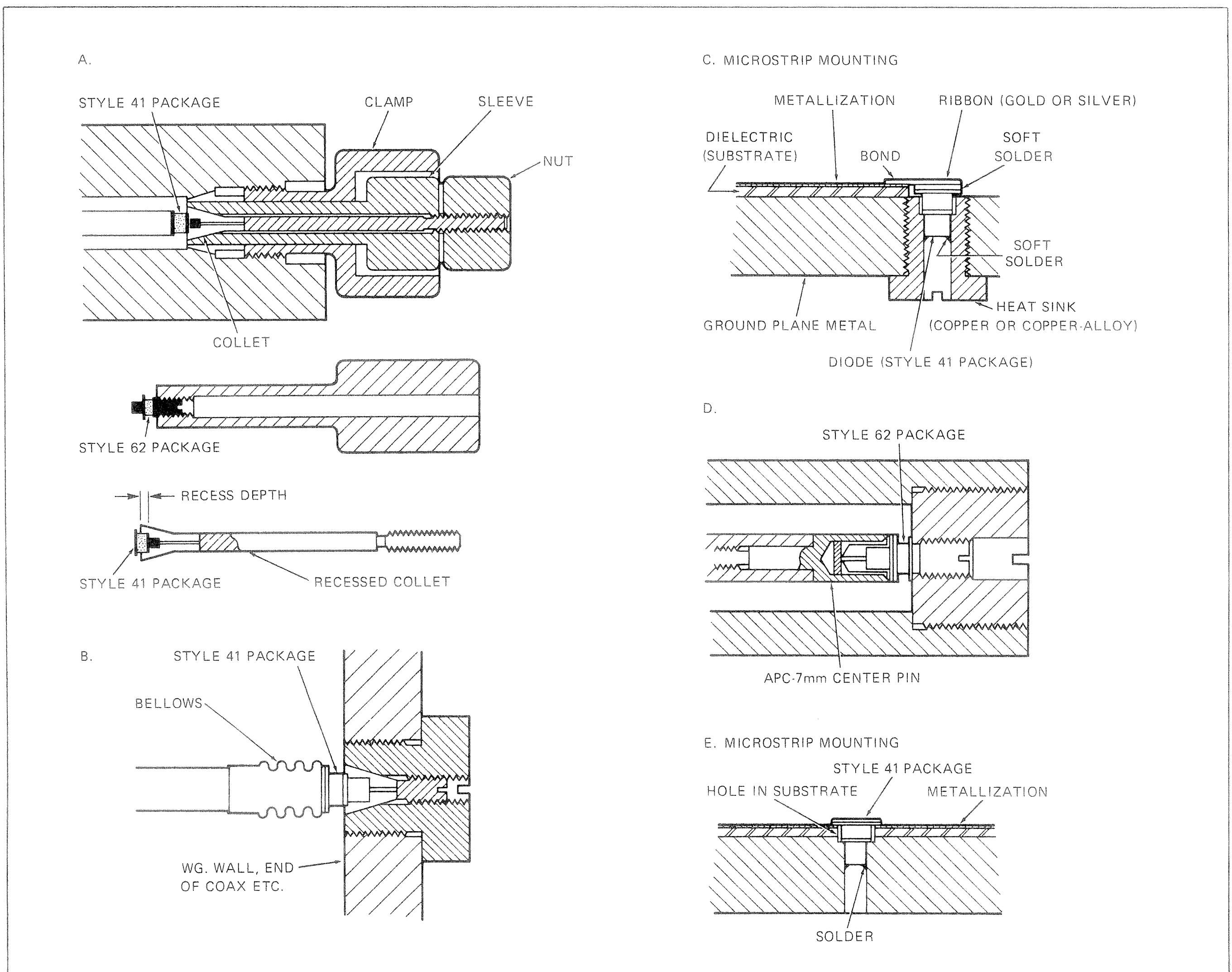

Fig. 10. Typical Diode Mounting Techniques.

accept the screw stud as in Fig. 10D; in general, the screw stud provides a somewhat inferior heat flow path compared to the soldered unthreaded stud.

Figs. 10C and 10E show two ways of mounting an HP Style 41 package in a microstrip circuit. In both cases the package stud is soldered into the ground plane.

Figs. 10B and 10D show two ways of making contact to the cap (cathode) end of the package. Fig. 10D shows simply the center conductor pin assembly from a APC-7 precision 7 mm connector (Amphenol Part #131-1054). Fig. 10B shows a bellows, which can be soldered to the package cap, if desired. An alternative to these methods, which is acceptable in many cases, is simply a pressure contact provided by rigid mounting of the diode stud such as to press the diode package against the cathode contact.

C) *Thermal Resistance Measurement*

The mount for an IMPATT diode, whether it be one of those described in the last section or not, must provide an adequate heat flow path away from the diode stud. The total thermal resistance (θ_T) for a diode in its mount is the sum of the junction-to-case thermal resistance of the diode itself, θ_{jc}, and the thermal resistance of the mount or cavity, θ_{cav}. Values of θ_{jc} for the various HP IMPATT diodes are listed in Table II; the *space charge* resistance, R_{SC}, which will be discussed later in this section, is also listed.

TABLE II: Thermal Resistance of HP IMPATT Diodes

MODEL #	θ_{jc} (°C/W)		R_{SC} (typical) Ω
	TYPICAL	MAXIMUM	
5082-0400	15.0	16.0	32
-0401	16.0	17.0	22
-0431,4,7	20.0	35.0	65
-0432,5,9	25.0	35.0	85
-0433,6,9	30.0	35.0	55

Fortunately, it is relatively easy to determine the total thermal resistance (θ_T) of a diode and its mount, using instruments readily available in most laboratories. The method was first described by Haitz, *et.al.*[6], and a simplified version will be described here.

The measurement method relies on the fact that the avalanche breakdown voltage of any pn junction depends strongly on the junction temperature. This dependence can be carefully calibrated and used as a sensor for measuring the junction temperature while DC power is being dissipated in the diode. The ratio of the temperature rise to the dissipated DC power is the thermal resistance. To derive the needed relationship between θ_T and the measured parameters, we will start with Fig. 11. The graph in Fig. 11 depicts the DC current-versus-voltage (VI) characteristic of a reverse biased IMPATT diode. At a given value of current, I_{DC}, the voltage drop in the diode can be thought of as consisting of three components: 1) The breakdown voltage

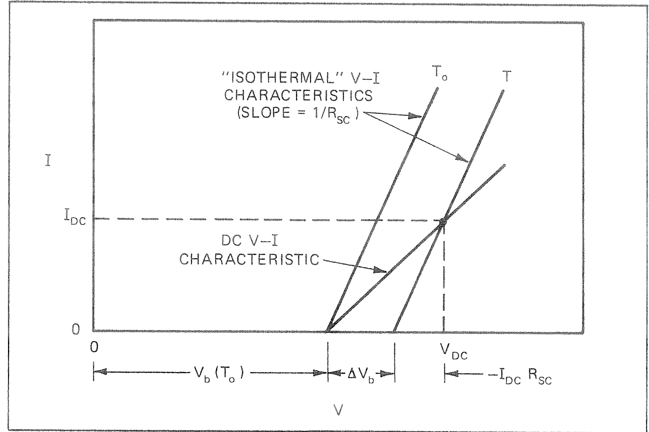

Fig. 11. Static (DC) Current-Voltage Characteristic of an IMPATT Diode, Showing the Contributions Due to Junction Heating (ΔV_b) and the Resistive Drop, $I_{DC} R_{SC}$, in the SPACE CHARGE RESISTANCE.

of the diode at the ambient temperature, V_b (T_o); 2) The rise in the breakdown voltage, ΔV_b, caused by the junction heating; 3) A resistive voltage drop, I_{DC} R_{SC}, where R_{SC} is called the "space-charge resistance". R_{SC} is the incremental resistance that would be measured in the absence of thermal effects, e.g. by a fast pulse or high frequency sine wave. For temperatures between 25°C and 100°C, ΔV_b is directly proportional to the temperature rise in junction, ΔT. Furthermore, the constant of proportionality is itself proportional to the room temperature breakdown voltage, V_b (25°C); we can hence write

$$\Delta V_b = \beta V_b\,(25°C) \cdot \Delta T \tag{5}$$

The constant, β, is 1.17×10^{-3} °C^{-1} for HP IMPATT diodes. So, for example, if V_b (25°C) = 80.0 V for a particular diode, then V_b would increase $1.17 \times 10^{-3} \times 80.0 = 93.5$ mV for each °C rise in the junction temperature. By definition, ΔT is given by

$$\begin{aligned}\Delta T &= \theta_T \; P_{DISS} \\ &= \theta_T \cdot V_{DC} \cdot I_{DC}\end{aligned} \tag{6}$$

where P_{DISS} is the DC power dissipated in the diode. Referring to Fig. 11 and using (5) and (6) to obtain ΔV_b, the total voltage V_{DC} across the diode for T_o = 25°C is:

$$V_{DC} = V_b\,(25°C) + \theta_T\, V_{DC}\, I_{DC}\, \beta V_b\,(25°C) + I_{DC}\, R_{SC} \tag{7}$$

Solving for θ_T we get

$$\theta_T = \frac{V_{DC} - V_b\,(25°C) - I_{DC}\, R_{SC}}{V_{DC}\, I_{DC}\, \beta V_b\,(25°C)} \tag{8}$$

Thus, in order to measure θ_T, one must measure I_{DC}, V_{DC}, and R_{SC}. A milliameter and a digital voltmeter capable of ± 0.5 mA and ± 0.1 V resolution, respectively, are needed for measuring I_{DC} and V_{DC}. The measurement of R_{SC} is done with either fast (~100 nS) pulses, or with a sine wave at 2.0 MHz or higher; the thermal time constants of the

IMPATT diode are such that the junction cannot respond thermally to fast pulses or high frequency sine waves, and hence a measurement of the incremental resistance of the diode using either of these techniques gives R_{SC}.

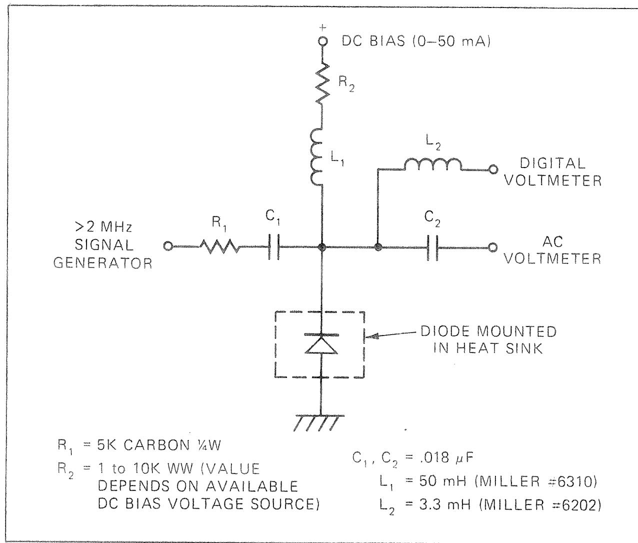

Fig. 12. Circuit Diagram for Measurement of IMPATT Diode Thermal Resistance.

Fig. 12 shows a block diagram of a measurement circuit suitable for measuring V_b (25°C), V_{DC}, I_{DC} and R_{SC}, using a milliameter, digital voltmeter, signal generator and ac voltmeter. The R_{SC} measurement is calibrated by inserting a carbon resistor of approximately the value expected for R_{SC} in place of the diode, and adjusting the signal generator for a convenient reading on the ac voltmeter. Table II lists typical values of R_{SC} for HP IMPATT diodes. As an example, a 30 Ω resistor might be selected if an HP 5082-0400 diode is to be measured. The signal generator can be set such that the ac voltmeter reads 30 mV; then the reading in mV is numerically equal to R_{SC} in ohms. The diode can now be inserted in the mount in place of the resistor. The room temperature breakdown voltage V_b (25°C) is measured by adjusting the bias current to 0.5 mA and recording the digital voltmeter reading. Next, the bias current is adjusted to a high enough value to raise the junction temperature 50 to 75°C. (For the HP 5082-0400/0401 diodes, 50 mA is a convenient value; 20-25 mA is suitable for the 5082-0430 series.) The digital voltmeter reading (V_{DC}) and R_{SC} are now recorded. The data are inserted in Eq. (8), and θ_T is obtained.

EXAMPLE:

The following measurement data was obtained on a typical HP 5082-0400 IMPATT diode mounted in a 1" x 3" x 3" OFHC copper block using the diode holder shown in Fig. 10A:

V_{DC} (0.5 mA) - 76.1 V (= V_b (25°C))

V_{DC} (50.0 mA) - 83.6 V

R_{SC} (5 MHz) - 31 Ω

Insertion of the data in Eq. (8) gives θ_T:

$$\theta_T = \frac{83.6 - 76.1 - .05 \times 31}{83.6 \times (.05) \times (1.17 \times 10^{-3}) \times 76.1} = 16.0°C/W$$

There are several important points that should be mentioned in connection with thermal resistance measurements:

1) During thermal resistance measurements, the diode *must not be permitted to oscillate*; the presence of an RF voltage across the diode can affect the values of V_{DC} and R_{SC} sufficiently to cause errors of the order of 50% in the determination of θ_T.
2) The value of θ_T measured with any heat sink will be larger than the junction-to-case thermal resistance, θ_{jc}. For example, the heat sink used in the above example is the standard test mount used at HP, and has a thermal resistance of 1.5 - 2.0°C/W, depending somewhat on the torque applied in tightening the diode holder clamp and collet. Hence θ_{jc} for the diode in the example is 14.0 - 14.5°C/W.
3) After a θ_T measurement, the junction temperature during measurement should be checked to be sure it has not exceeded 100°C. This is necessary because the linear relationship between ΔT and ΔV_b (Eq. (5)) does not hold accurately for temperatures much above 100°C. If this precaution is not observed, values for θ_T which are smaller than the true values will be obtained. In the example above we find T_j (max) as

$$\begin{aligned} T_j \text{ (max)} &= 25 + V_{DC} I_{DC} \theta_T \\ &= 25 + 83.6 \times .05 \cdot 16.0 \\ &= 92°C \end{aligned}$$

4) R_{SC} should be measured with the bias current I_{DC} flowing in the diode (50 mA in the above example). The error in θ_T incurred if this is done at lower currents can be of the order of 10%, due to the small but significant dependence of R_{SC} on junction temperature, and due to non-uniformity of the avalanche breakdown current at currents less than 10 mA.
5) In measuring θ_T, sufficient time should be allowed for the heat sink to reach thermal equilibrium with its environment before reading V_{DC}. Otherwise an erroneously low value of θ_T will be obtained.

The alternatives to the scheme shown in Fig. 12 mainly involve the method of measuring R_{SC}. Two other methods have been used at HP. In the first, the sine wave generator and R_1 are replaced by an HP 214A pulse generator, and the ac voltmeter is replaced by a fast (>20 MHz) oscilloscope. A 100 nS pulse is used to measure R_{SC}, with I_{DC} flowing, using the same method of system calibration as was described above. The second alternative is to eliminate the signal generator and the R_1, C_1 branch, and to replace the ac voltmeter with an HP 4815A RF Vector Impedance Meter*, which measures R_{SC} directly. The choice

*The Vector Impedance Meter will withstand a maximum of 50 VDC and 5 VAC (rms). Care must be taken during measurements to avoid exceeding these ratings.

of these alternatives is dictated mainly by equipment availability; their accuracies are comparable.

D) *Bias Circuits*

Since in the avalanche breakdown mode the IMPATT diode tends to behave as a constant voltage device, it requires a constant-current DC bias source. A further consideration in biasing the IMPATT is bias circuit stability; there exists a fairly complicated interaction between the "RF" and "bias port" impedances of an IMPATT diode. As a consequence, the circuit presented to the bias port affects the RF performance of the diode, and vice-versa. Under certain conditions, oscillations in the bias circuit are possible; these can be avoided by proper bias circuit design.

The requirement for constant-current DC bias is conveniently met in the laboratory with a large resistor and a high voltage power supply. A typical bias circuit is shown in Fig. 13A. The 5 kΩ resistor (R_3) isolates the DC voltmeter from the bias circuit; this is necessary in most cases because the high input capacitance of DC VTVM's causes bias circuit instabilities in the absence of sufficient isolation. The function of R_2 is to provide a frequency-independent series resistance in the bias path; wirewound resistors are normally highly capacitive at high (>5 MHz) frequencies and can also cause bias circuit instabilities if used alone.

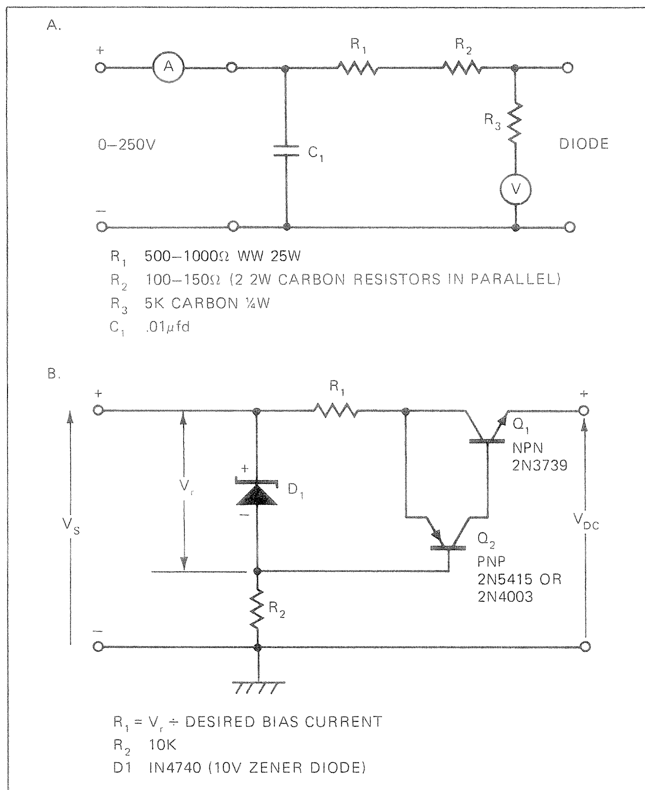

Fig. 13. Some Typical Bias Circuit Designs for IMPATT Oscillators. (A) Laboratory Bias Circuit. (B) Transistor Current Regulator Circuit.

The laboratory bias circuit of Fig. 13A is unattractive for most practical system applications because it requires a high voltage supply, and wastes a great deal of power in the series resistors. A transistor current regulator of the type shown in Fig. 13B is the best solution for most practical cases. This circuit functions by forcing the voltage across R_1 to be equal to the reference voltage V_r; this forces the load current to be constant at V_r/R_1. The reference voltage V_r can be the voltage across the zener diode as shown, or in a less critical application where economy is essential, it can be the forward voltage drop across two or three pn junction diodes in series. In a critical application where very accurate regulation is required, a temperature compensated regulated voltage source might be used as the reference. In the next several paragraphs we will discuss some design considerations relating to this current regulator circuit.

Referring to Fig. 13B, the supply voltage, V_S, diode voltage V_{DC}, and collector-to-emitter voltage, V_{CE}, of Q_1 are related by the equation

$$V_S = V_{DC} + I_{DC} R_1 + V_{CE}$$

Since $I_{DC} R_1 \approx V_r$ for proper regulator operation, we can rewrite this as

$$V_S = V_{DC} + V_r + V_{CE} \tag{9}$$

From this equation one can calculate a "worst case" value for V_{CE} if the maximum V_S and minimum V_{DC} are known. This sets the minimum value of V_{CE} (max) for the transistors. The required minimum power dissipation for Q_1 is the product of I_{DC} and the largest expected value of V_{CE} from Eq. (9). It is also of interest to note that the minimum value of supply voltage for proper operation is approximately $V_r + V_{DC} + 2$, allowing about two volts for V_{CE} at the required bias current. The operating voltage V_{DC} for an IMPATT diode at any ambient temperature, T, can be estimated from the relation

$$V_{DC} = V_b\,(25°C)\left[1 + \beta\,(T - 25) + \beta P_{DC}\,\theta_T\right] + I_{DC}\,R_{SC} \tag{10}$$

where P_{DC} is the dc power dissipated in the diode and θ_T is the thermal resistance of the diode in its mount. The value of β is $1.17 \times 10^{-3}\ °C^{-1}$.

EXAMPLE:

Let us estimate the operating voltage range of an HP 5082-0400 IMPATT diode from −30°C to +60°C, in a mount with θ_T = 20°C/W, $I_{DC} \simeq$ 90 mA, and $P_{DC} \approx$ 8 W. The value of V_b (25°C) for this diode is typically 78 V, (from Table I) and R_{SC} is typically 32 Ω, (from Table II):

$$V_{DC}\,(-30°C) = 78\left[1 + 1.17 \times 10^{-3} \times (-55) + 1.17 \times 10^{-3} \times 8 \times 20\right] + .09 \times 32 \approx 91\ V$$

$$V_{DC}\,(+60°C) = 78\left[1 + 1.17 \times 10^{-3} \times (+35) + 1.17 \times 10^{-3} \times 8 \times 20\right]$$

$+ .09 \times 32$

≈ 99 V

The operating voltage of the diode will vary from 91 to 99 V over the temperature range −30°C to +60°C. Accordingly, if V_r = 10 V as in Fig. 13B, and we allow 2 volts for V_{CE} of Q_1, the minimum power supply voltage required is 99 + 10 + 2 = 111 V. If the DC power supply is designed to provide 115 V, then at the lowest operating temperature V_{CE} will be 115 − 10 − 91 = 14 V. Conservative design would dictate a transistor with V_{CE} (max) of about 30 V, and for I_{DC} = 90 mA a dissipation rating (at −30°C) of at least 3 watts (roughly twice the expected dissipation). The transistor Q_2 must have the same voltage rating but its power rating is smaller than that of Q_1 by a factor roughly equal to the dc current gain of Q_1.

In the circuit example above, an ambient temperature will be reached at which the diode voltage will become so high that Eq. (9) can no longer be satisfied. Then the circuit can no longer regulate and the current to the diode will decrease, being given by $(V_S - V_{DC})/R_1$. This feature can be used to automatically decrease DC power to a diode if the ambient temperature exceeds a given equipment design limit. In the above example, this occurs at about 100°C; it will occur sooner if V_S is chosen to be smaller.

As discussed above, the design of the bias circuit can affect the RF performance of the IMPATT diode, particularly at high power and bias current levels. In general, the ideal "termination" for the bias port is a large frequency-independent resistor. The worst termination is a large capacitor. Another undesirable condition is that in which, at some frequency, the bias circuit has a high Q series resonance to ground; this situation can easily arise from lead inductance and stray capacitance in the bias circuit. In this case, bias circuit oscillations can occur at the frequency of the series resonance. Some examples of the output spectra of oscillators with bias circuit instabilities are shown in Fig. 14. The circuit is that of Fig. 37, set up for 12 GHz operation with an HP 5082-0401 diode as shown in Table III. Fig. 14A shows the spectrum of the oscillator with a bias circuit similar to that of Fig. 13A. In Fig. 14B a capacitor (.002 μf) has been connected directly across the diode to ground. In Fig. 14C, the capacitor has been connected from the node between R_1 and R_2 (Fig. 13A) to ground; the presence of R_2 between the diode and the capacitor has completely suppressed the instability (noise in this case). In Fig. 14D, a section of open circuited BNC cable has been connected in shunt across the bias port of the diode. This cable in combination with the bias T is series resonant at 14 MHz and causes a bias circuit oscillation at the same frequency. The oscillation in the bias circuit frequency — modulates the RF output producing the sidebands shown in the spectrum. Connecting the cable from the node between R_1 and R_2 to ground, as in the case of Fig. 14C, suppresses the instability. The spectra shown were obtained at an output power of 600 mW, with about 10 W input. At lower input powers, below 8 W or so, the gross spectrum is relatively insensitive to the bias circuit. However, a large (>0.1 μfd) capacitor is observed to seriously degrade the oscillator noise. It should be remarked at this point that it is important *not* to connect the bias circuit to the diode with an intervening coaxial cable; the cable capacitance can cause instabilities such as were just shown. The bias circuit should be physically immediately adjacent to the oscillator bias port.

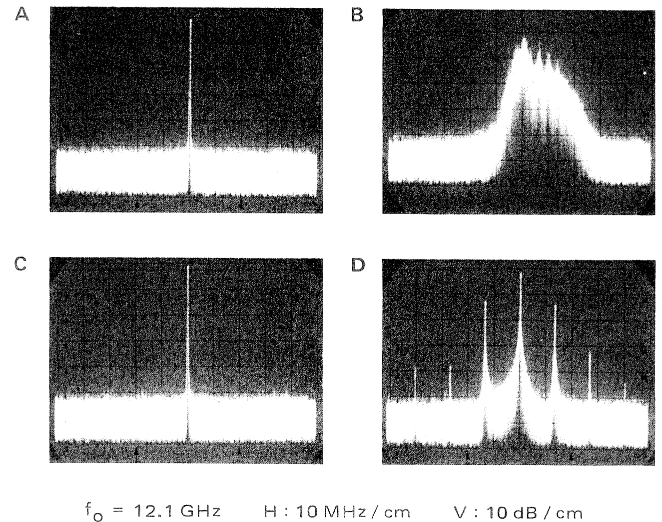

Fig. 14. Effects of Improper Bias Circuit Design on IMPATT Oscillator RF Spectrum. (A) Normal Spectrum. (B) .002 μfd Capacitor From Bias Port to Ground. (C) 100 Ω Carbon Resistor Between Bias Port and .002 μfd Capacitor to Ground. (D) Resonant Bias Circuit.

The considerations presented in the preceding paragraph illustrate the importance of proper bias circuit design in IMPATT oscillators. In particular, the importance of a resistive bias port termination is shown. The instabilities shown in Fig. 14 are extreme cases which have been purposely induced to show the effects of improper bias circuit design. In general, these instabilities are the most troublesome in higher power diodes operated near their maximum power capabilities. In lower power (P_o < 300 mW) oscillators, the bias circuit is much less critical, and the requirement for a resistive termination at the bias port is relaxed considerably. As discussed in the next section and in VII.C., the RF loading on the diode also has a strong effect on the onset of RF and bias circuit instabilities.

E) *Operating Precautions*

There are a number of precautions which must be observed in the operation of IMPATT diodes in order to avoid diode damage or burnout.

First, the junction temperature T_j of the diode should not exceed 200°C for long periods of time. Diodes can tolerate $T_j \simeq 275$°C for a matter of hours without damage or degradation, but over extended times, operation much above 200°C can substantially reduce diode operating life. It is recommended that, in experimental circuits, the thermal resistance of the diode in its heat sink be measured according to the method outlined in Section III.C. Then

the junction temperature can be calculated from

$$T_j = T_A + (P_{DC} - P_o) \times \theta_T \qquad (11)$$

where P_{DC} is the input power and P_o is the microwave output power.

Before connecting the diode cavity and its bias circuit to the DC supply, the supply voltage should be set to zero. After the DC connections have been made, the power should be applied slowly. No current should flow until the breakdown voltage is reached; see Table I for typical values. At some point after current flow has started, RF power will be obtained. This point depends greatly on the RF loading.

A spectrum analyzer is very helpful in the initial investigation of IMPATT diode circuits. It is particularly valuable in the identification of RF instabilities, such as shown in Fig. 14. The presence of RF instabilities, in addition to being undesirable from a performance point of view, can often lead to diode failure. There are two reasons for this. First, a large bias circuit oscillation can itself dissipate more power in the diode than it can safely handle; second, diode instabilities can cause the diode to switch very rapidly to a low voltage mode, in which large currents can be drawn from the power supply or from stray capacitances in the bias circuit. As mentioned above, instabilities are related not only to the bias circuit but to the RF loading as well. In general, instabilities can take place when the peak RF voltage across the diode approaches about ½ the breakdown voltage. In an amplifier or oscillator, the diode peak RF current and voltage can be estimated if the value of the load resistance R_L is known; the necessary equations are presented in Section V, Part B.

Particular care should be exercised during tuning or loading adjustments in an adjustable cavity. Until some "feel" for a circuit is developed, these adjustments are best made at reduced power. The spectrum analyzer is an invaluable aid, as mentioned above.

Intermittent DC connections must be avoided; these cause transients which can destroy diodes. Changes in the bias circuit should only be made after the DC power source has been turned down to zero.

IV. Broadly Tunable Circuits

This section will describe two broadly tunable coaxial circuits which are useful laboratory tools for the study of IMPATT diode properties. The first is a multiple slug-tuned cavity of the type described by Iglesias[7]; this cavity is the more flexible of the two. The second utilizes a method of varying the package inductance; while somewhat less flexible than the slug-tuned cavity, it offers the advantage of yielding more readily understandable results and single-adjustment tuning.

A waveguide circuit is also discussed. It is not as broadly tunable as the others, but is capable of much higher Q, better frequency stability, and much lower FM noise. This circuit is suitable as a local oscillator or parametric amplifier pump in many systems applications.

A) *Multiple Slug Tuned Cavity; Bias T*

The basic circuit problem in operation of IMPATT diodes as oscillators is to provide a load reactance which is equal to the negative of the diode's reactance at the desired frequency of oscillation, and a load resistance which satisfies the condition shown in Fig. 5, namely that R_L be equal to the magnitude of the diode's net negative resistance, R_D, at the desired operating point. In a tunable IMPATT circuit, achievement of the optimum R_L at any desired frequency requires at least two adjustable circuit elements, and more than two for maximum circuit flexibility. The multiple-slug-tuned cavity shown in Fig. 15 achieves this adjustability by the movement of impedance-transforming "slugs" inside a 7 mm coaxial line which is slotted to allow movement of the slugs. The design of circuits of this type is discussed in the MIT Radiation Laboratory Series, Vol. 9, [8]; the use of the circuits for IMPATT diode operation has been reported by Iglesias[7].

Fig. 15 shows the important construction details of the multiple slug cavity*. Depending on the desired center frequency of operation, slugs with various lengths and impedances can be used. In general, slugs λ/8 and λ/4 long at the desired center frequency of operation, with characteristic impedance of between 10 and 20 Ω provide maximum

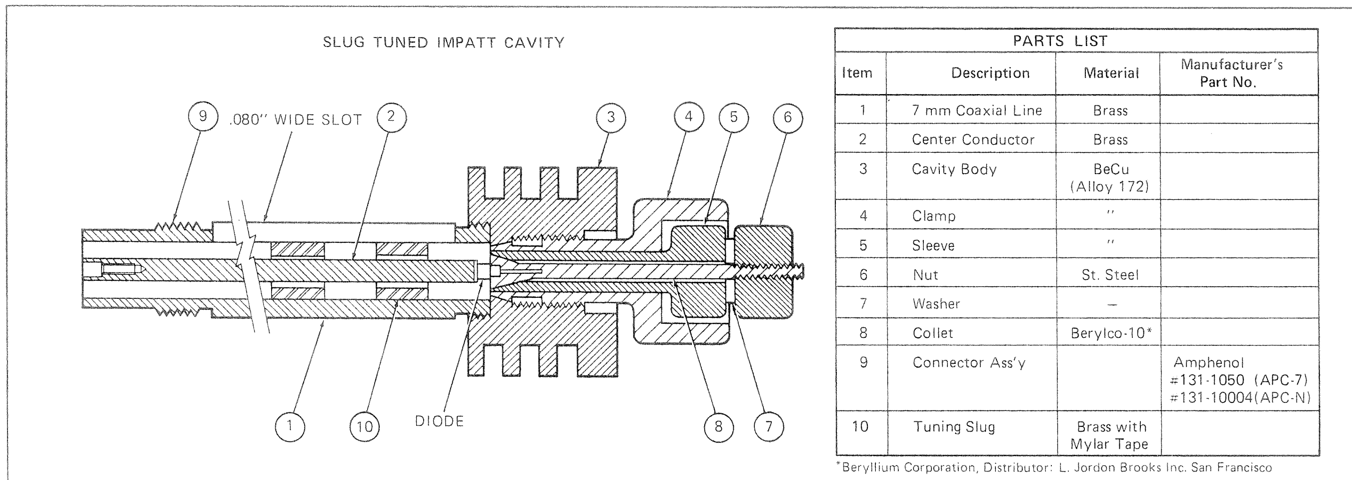

PARTS LIST

Item	Description	Material	Manufacturer's Part No.
1	7 mm Coaxial Line	Brass	
2	Center Conductor	Brass	
3	Cavity Body	BeCu (Alloy 172)	
4	Clamp	"	
5	Sleeve	"	
6	Nut	St. Steel	
7	Washer	–	
8	Collet	Berylco-10*	
9	Connector Ass'y		Amphenol #131-1050 (APC-7) #131-10004(APC-N)
10	Tuning Slug	Brass with Mylar Tape	

*Beryllium Corporation, Distributor: L. Jordon Brooks Inc. San Francisco

Fig. 15. Cross Section and Parts List for a Multiple-Slug-Tuned IMPATT Circuit.

flexibility. Two, three, or four slugs can be used. The outer surface of each slug is covered with Mylar tape so that it will slide smoothly in the 7 mm coax line. The surface can also be Teflon-coated; this service is now available from commercial vendors**.

Movement of the slugs can be accomplished either by use of the Teflon adjusting rings shown in the photo of Fig. 16 or by simply inserting a plastic probe into the slot to move the slugs. The adjusting rings allow the slugs to be locked in place by tightening the screw.

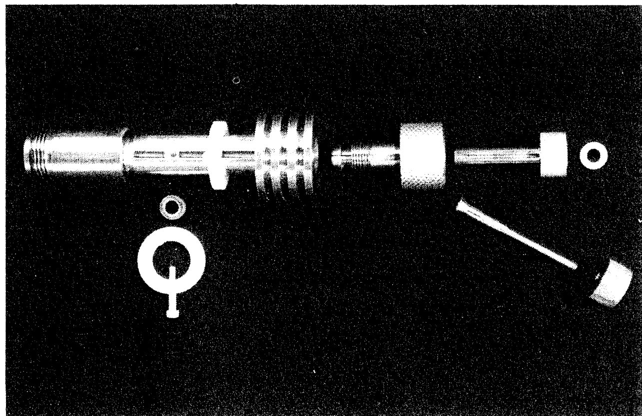

Fig. 16. Photograph of Disassembled Slug-Tuned Circuit.

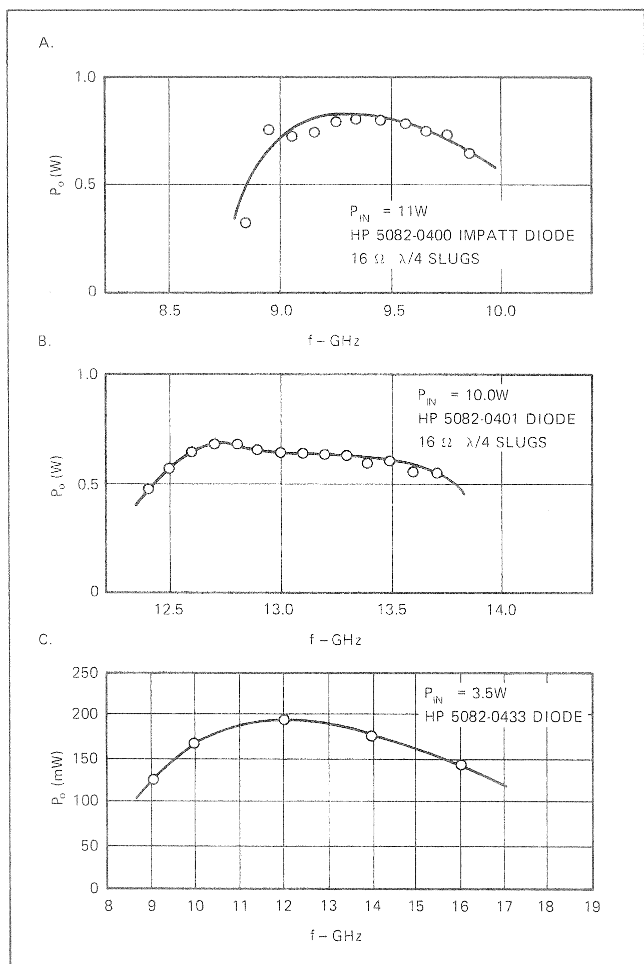

Fig. 17. Typical Data Obtained in Slug-Tuned Cavities.

Some typical data taken in multiple slug cavities are shown in Fig. 17. The data shown in Fig. 17B were taken with an HP 5082-0401 diode mounted in a collet which *recesses* the diode back into the ground plane. This collet appears on the upper right in the photo of Fig. 18 and is also shown in the diode holder assembly detail of Fig. 10A. Recessing the diode package in this way reduces the package inductance significantly, making operation at higher frequencies more convenient.

The data of Fig. 17C were taken with the HP 5082-0433 diode. Tuning was accomplished with three slugs. This diode has lower capacitance than the 5082-0400/1 diodes, and is hence quite a bit easier to tune over a wide range. Its output power capability is lower, in the 100-200 mW range.

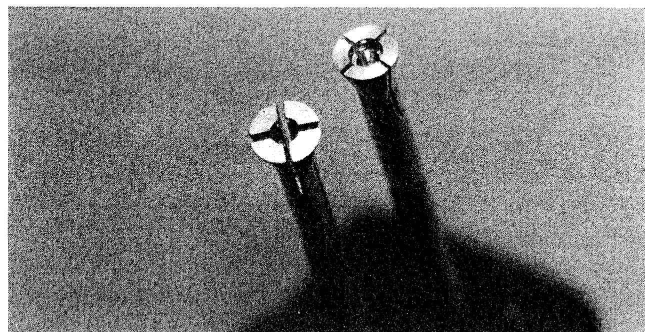

Fig. 18. Diode Collets; Recessed Collet Shown at Right.

A bias T is required for operation of the multiple slug cavity, as well as for some of the other cavities described in this Application Note. There are a few commercially available bias T's which can be used – the user is forewarned that some of these have a specified maximum DC bias current, often 100 mA; in some cases (e.g. with the HP 5082-0400/0401 IMPATT diodes) the diode will require more than 100 mA of bias current. A suitable high-current bias-T design is shown in Fig. 19; the "bucket chokes" are λ/4 long and are spaced λ/4 from the RF line center conductor and from each other, at 13 GHz. This bias T is designed for operation from 8 to 18 GHz and has a VSWR < 1.10 over that range; its insertion loss over that range is also very low, typically less than 0.3 dB. It can be used readily at lower frequencies but with somewhat worse VSWR; for operation with an adjustable circuit like the multiple slug cavity, this VSWR can easily be tuned out. If desired, the "bucket choke" dimensions and spacing can also be scaled to a lower frequency. The DC current handling capability of this bias T is adequate for any IMPATT diode biasing requirements. The maximum permissable current has not been established, but is well in excess of 500 mA; the fusing current for the silver wire is given as about 5 amperes in Reference 9. A photo of the internal construction of the Bias T is shown in Fig. 20.

*Detailed drawings for this cavity are available from your HP field sales office as HP Publication No. 5952-0261. See Appendix A for a complete list of available IMPATT Circuit Drawings.

**e.g. Fluorocarbon, Inc., Mountain View, California.

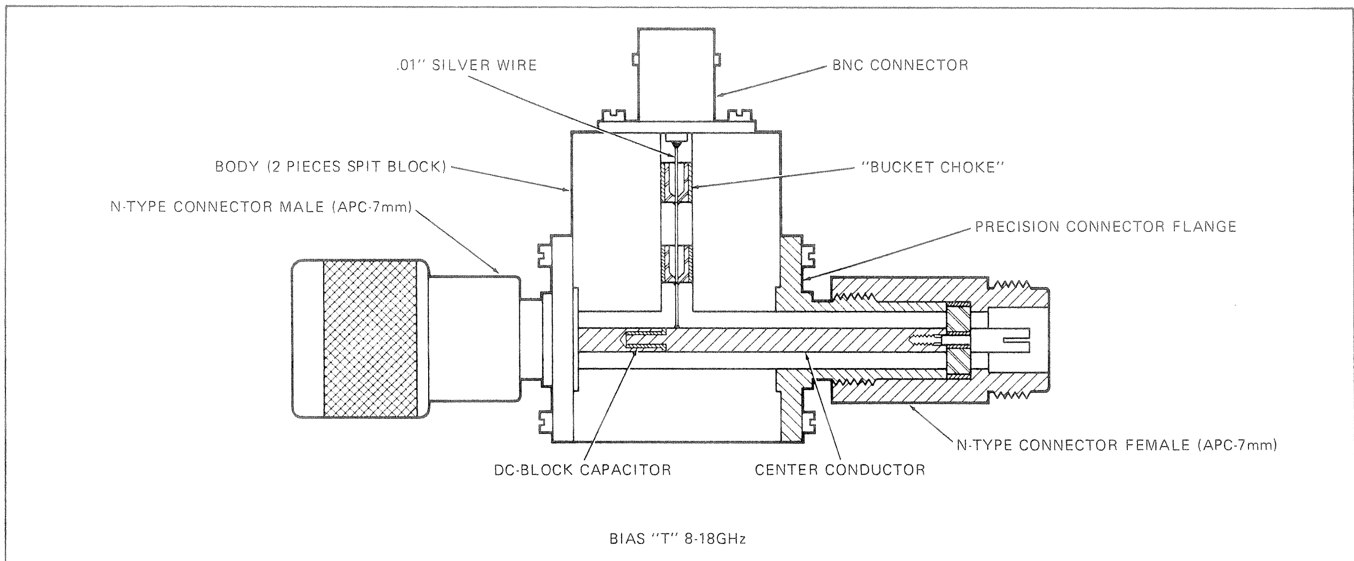

Fig. 19. High-Current Bias T Used With Slug-Tuned and Other Coaxial Cavities.

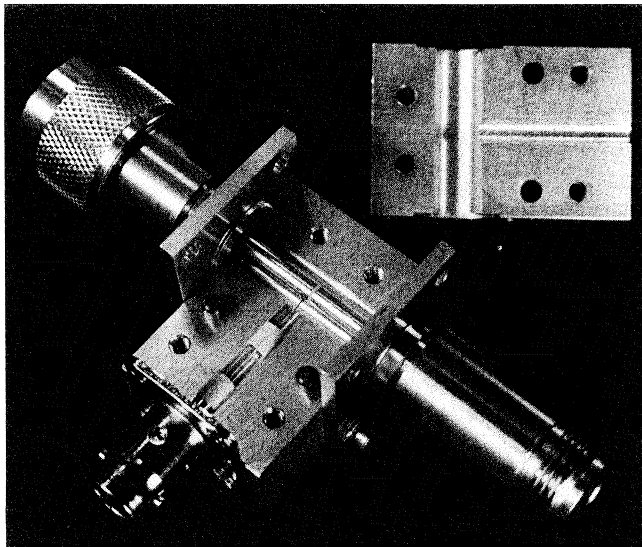

Fig. 20. Photo of Bias T With Front Cover Removed, Showing "Bucket" Chokes and DC Blocking Capacitor.

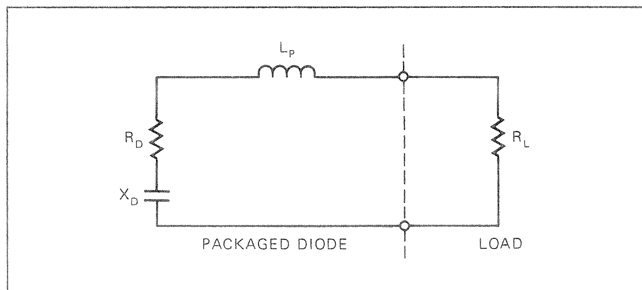

Fig. 21. Equivalent Circuit For the Case Where the Package Inductance is Used to Resonate the Chip Capacitance.

B) *Variable Inductance Tunable Coaxial Circuit*

A simple IMPATT oscillator circuit is shown in Fig. 21; it is derived from Fig. 9A by adding a resistive load R_L and neglecting C_p. The frequency of oscillation of this oscillator is determined by the resonant frequency of L_p and X_D; since the behavior of X_D vs. f is determined by the characteristics of the chip itself (and to a small extent by the bias current) the only chance of tuning the oscillator over a significant range is by varying L_p. It seems strange at first to talk about changing the package inductance, since this is ordinarily thought of as a parameter fixed by the choice of the package. However, it is in fact the case that L_p is not unique to a given package, but can be varied by changing the geometry of the circuit surrounding the diode; one way of achieving this is shown in Fig. 22A. Here the diode package is end-mounted in a coaxial line in such a way that the package can be recessed into the ground plane in an adjustable manner; the diode is shown recessed fully in Fig. 22B. Recessing the diode decreases the inductance considerably; Fig. 22C shows some typical data of L_p versus the depth of recess, ℓ_R, for a recess diameter just large enough to accommodate the ceramic body of the diode package (*hpa* Style 41 in this case). Fig. 23 shows a practical realization of this tuning technique. The diode holder and clamp is of the same type used for the slug-tuned cavity described in the last section, with a modification allowing the diode collet and sleeve to be moved back and forth inside the clamp. While tuning the oscillator the clamp is loosened just enough to allow the sleeve to be moved by turning the tuning screw. When the desired frequency is obtained, the clamp is tightened to ensure good thermal and RF contact between the sleeve and the cavity body. This oscillator, as shown, requires a bias T for operation.

The transformer reduces the 50 Ω line impedance to the value of R_L required for optimum power output of the IMPATT diode, usually in the vicinity of 2 Ω. The transformer used is a *maximally flat* two section design; this provides the optimum diode impedance over a wider frequency range than a single λ/4 section design, and is no more difficult to design or build. Fig. 24 shows the design information needed to build two section transformers to transform a line impedance Z_o to any value of R_L. The

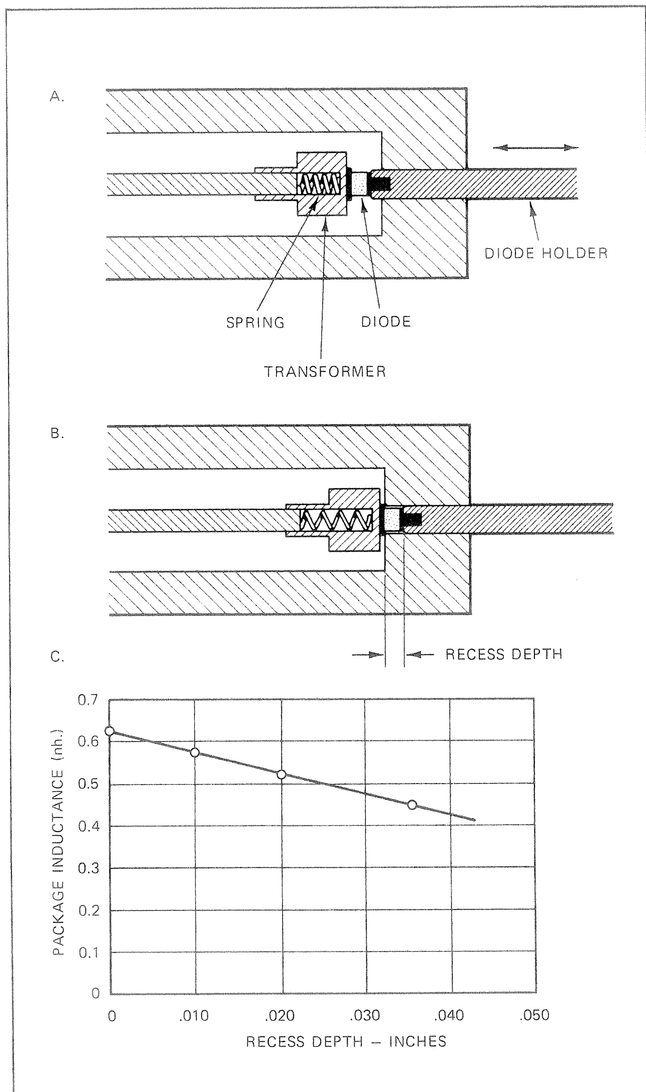

Fig. 22. Effect of Recessing Diode on Package Inductance; The Data is For HP Style 41 Package.

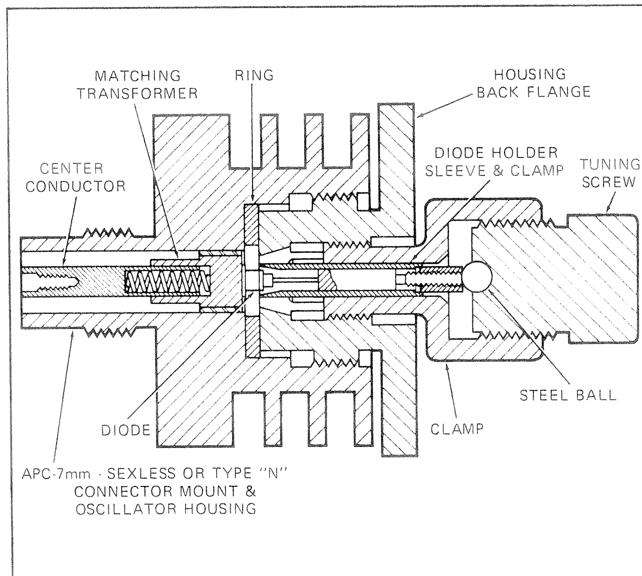

Fig. 23. Tunable IMPATT Diode Circuit, In Which the Diode Recess Can Be Varied.

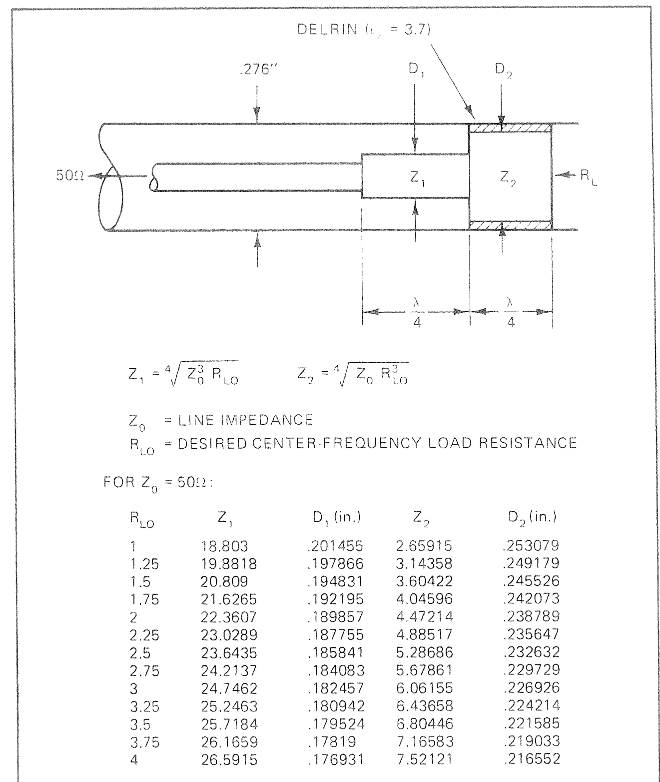

$$Z_1 = \sqrt[4]{Z_0^3 R_{LO}} \qquad Z_2 = \sqrt[4]{Z_0 R_{LO}^3}$$

Z_0 = LINE IMPEDANCE

R_{LO} = DESIRED CENTER-FREQUENCY LOAD RESISTANCE

FOR Z_0 = 50Ω:

R_{LO}	Z_1	D_1 (in.)	Z_2	D_2 (in.)
1	18.803	.201455	2.65915	.253079
1.25	19.8818	.197866	3.14358	.249179
1.5	20.809	.194831	3.60422	.245526
1.75	21.6265	.192195	4.04596	.242073
2	22.3607	.189857	4.47214	.238789
2.25	23.0289	.187755	4.88517	.235647
2.5	23.6435	.185841	5.28686	.232632
2.75	24.2137	.184083	5.67861	.229729
3	24.7462	.182457	6.06155	.226926
3.25	25.2463	.180942	6.43658	.224214
3.5	25.7184	.179524	6.80446	.221585
3.75	26.1659	.17819	7.16583	.219033
4	26.5915	.176931	7.52121	.216552

Fig. 24. Two Section Coaxial Transformer for Broadband Matching of IMPATT Diode to 50 Ω Line Impedance. The Transformer Sections are a Quarter (Electrical) Wavelength at the Desired Center Frequency; the Equations or the Table Give the Appropriate Transformer Impedances for any Desired Value of R_L at the Center Frequency (Denoted by R_{LO}).

table lists the values of Z_1 and Z_2 needed to transform a 50 Ω 0.276" O.D. coaxial line to values of R_L between 1.0 and 4.0 Ω; in this case the diameter and length of Z_2 take into account the presence of the Delrin (ϵ_r = 3.7) support sleeve. Fig. 25 shows the behavior of R_L over the frequency range 7-13 GHz for two section matching transformer with 10 GHz center frequency, for several values of R_L at 10 GHz.

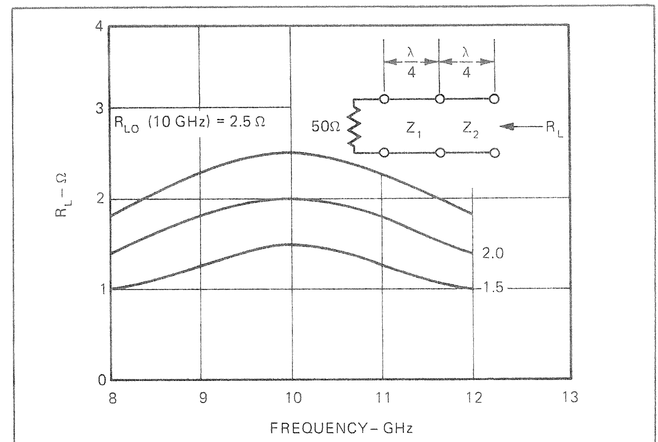

Fig. 25. Behavior of R_L vs. Frequency for a 2 Stage Transformer Designed at Center Frequency of 10 GHz for R_{LO} = 1.5, 2.0, 2.5 Ω.

This tunable oscillator design features single-adjustment tunability — an advantage in some cases. At the same time, however, it does not allow the optimum load impedance to be presented at each frequency as does the multiple-slug-tuned circuit. Typical performance is shown in Fig. 26; for this particular choice of R_L (1.25 Ω) performance is optimum below 10.5 GHz, but substantial power is still obtained up to nearly 12 GHz.

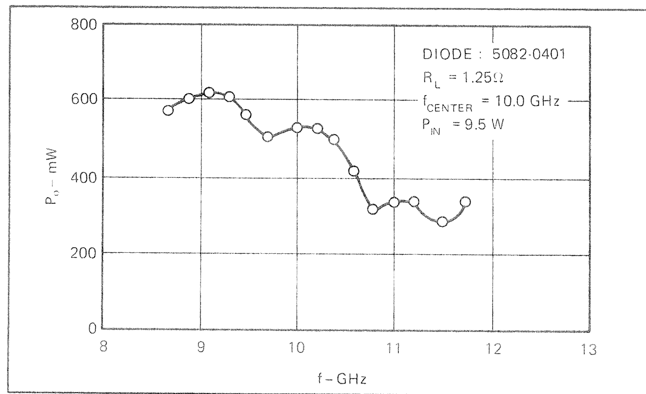

Fig. 26. Typical Data Obtained in the Variable-Inductance Tunable Circuit.

A photograph of the variable inductance oscillator is shown in Fig. 27. Detailed drawings for this circuit are available from the factory. (See Appendix A.)

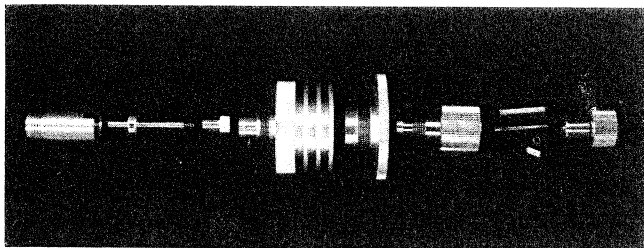

Fig. 27. Photograph of Tunable Coaxial Oscillator of Fig. 23, Disassembled.

C) *Tunable Waveguide Oscillator*

Fig. 28 shows a schematic illustration of a tunable waveguide oscillator. This particular oscillator has been designed for the frequency range of roughly 10.3-10.7 GHz. The version shown uses a commercial sliding short for tuning; the sliding short can be replaced by a fixed short and tuning screw if less tuning range is required. Typical performance of this oscillator is shown in Fig. 29 to 31. The diode used was an HP 5082-0435. The data of Fig. 30 were taken with a fixed short made of brass.

The AM noise of the oscillator in the configuration shown is more than 130 dB below the carrier in a measurement bandwidth of 100 Hz, independent of "distance from the carrier" (modulation frequency, f_m). The FM noise is also independent of f_m. The AM and FM noise are virtually independent of ambient temperature. This noise performance is within acceptable limits for most systems applications such as radar, telecommunications and telemetry receiver LO's, parametric amplifier and upconverter pumps, and low/medium power telecommunications transmitters. Other applications, such as intrusion alarms and police radar have requirements which are easily met with this oscillator; a fixed-tuned version, tailored especially for low-cost designs, is described in Section VI.B.

The frequency-temperature behavior is determined mainly by the expansion coefficient of the waveguide (brass in this case). Use of Invar would improve $\Delta f_o/\Delta T$ by a factor of about 10, to 1-2 ppm/°C.

The distance between the waveguide short and the disc/post assembly is very nearly $\lambda_g/2$. This is the primary frequency-determining factor in this oscillator. Adjustment of the post and disc dimensions mainly affect the circuit Q and the RF loading of the diode. In general, higher Q is obtained by *increasing* the post and disc diameters; the increase in Q is normally accompanied by a reduction in efficiency at any given bias level, due to increased cavity

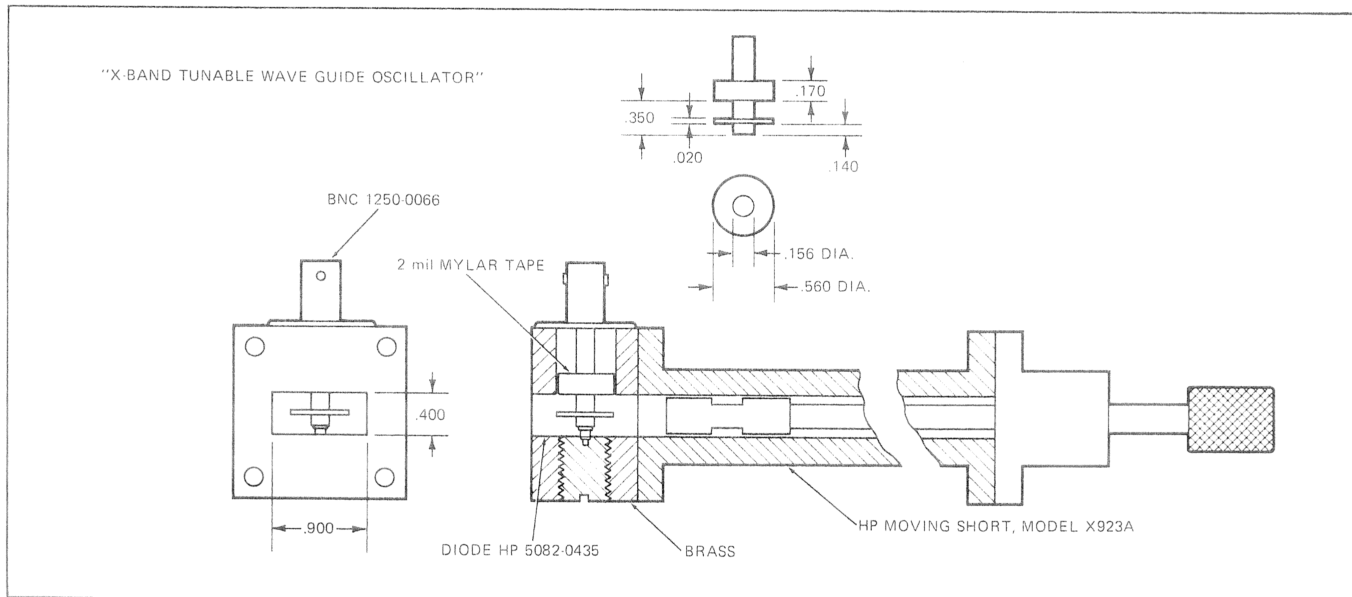

Fig. 28. Tunable Waveguide Oscillator.

losses. Circuit Q's of 2000 are achievable quite easily. A photograph of the oscillator is shown in Fig. 32.

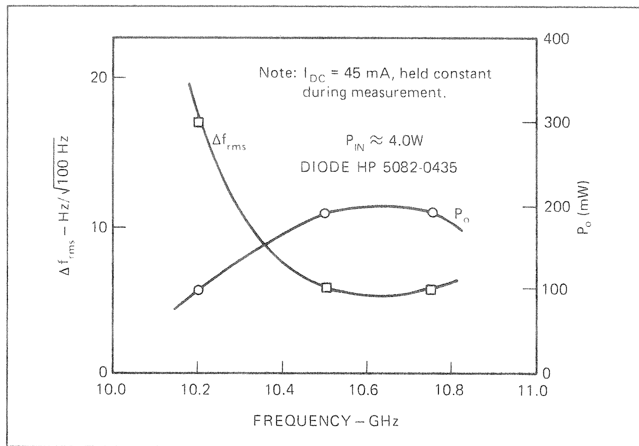

Fig. 29. Power Output and FM Noise Deviation vs. Frequency for the Tunable Waveguide Oscillator of Fig. 28.

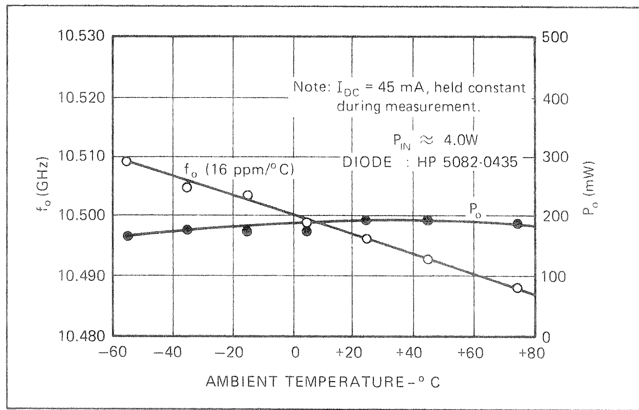

Fig. 30. Power Output and Oscillation Frequency of the Tunable Waveguide Oscillator, versus Temperature.

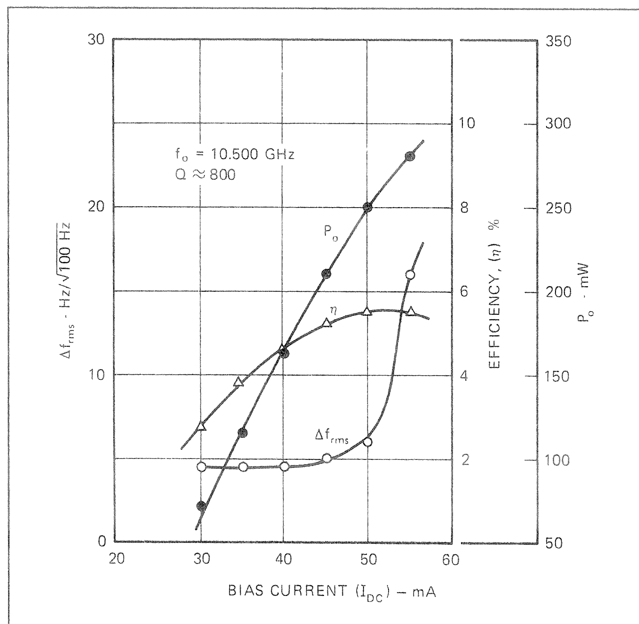

Fig. 31. Power, FM Noise, and Efficiency vs. Bias Current for the Tunable Waveguide Oscillator.

V. Low Q Fixed-Tuned IMPATT Oscillators and Amplifiers

The low Q fixed-tuned circuits described in this section represent the simplest possible IMPATT diode circuits. The only difference between these circuits as oscillators and amplifiers is in the choice of the real part of the load impedance, R_L, presented to the diode. As pointed out in the introduction (Fig. 5), an oscillator is required to satisfy $R_L + R_D = 0$; thus a value for R_L must be chosen such that there is an intersection between the $R = R_L$ line and the $R = -R_D$ curve for the IMPATT diode. An amplifier requires that there be *no* intersection of $R = R_L$ and $R = -R_D$; hence R_L must be *larger* than $|R_D|$ for all values of the RF current through the diode.

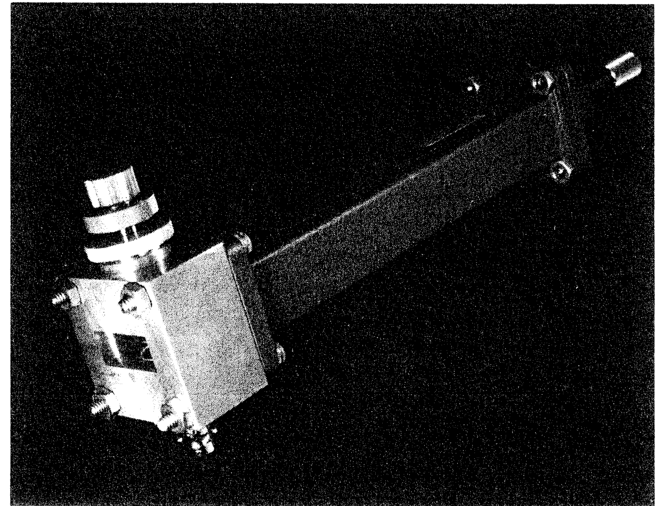

Fig. 32. Photograph of the Tunable Waveguide Oscillator.

Low Q oscillators have their primary use in applications where the frequency stability and noise characteristics of the diode can be controlled by injection phase-locking techniques. A typical application is the use of an injection phase locked oscillator as the final output stage in an FM telecommunications transmitter. The injection-locked oscillator functions as a power amplifier in this case. Another application is as an upconverter pump; here the frequency of the oscillator can be controlled by a low power, high-stability injection-locking signal such as a crystal-controlled oscillator/varactor multiplier or a high Q cavity-stabilized IMPATT oscillator. This arrangement is also suitable in a CW Doppler radar transmitter.

IMPATT amplifiers are also suitable as final power amplifiers in medium power CW transmitters. They can replace the currently-used traveling wave tube amplifiers in many cases. Power gains of 10 dB with 0.5 W output power and 1.0 GHz bandwidth are obtainable from the single-diode amplifiers described in Part B.

Part C discusses power combining techniques which can be used to obtain CW output powers in the several watt range by combining two or more separate IMPATT oscillators or by combining two or more diodes in a single oscillator.

The realization of low Q (10-30) fixed-tuned IMPATT oscillators and amplifiers in coaxial circuits is a straightforward matter. The most important design requirement is proper transformation of the transmission line impedance (usually 50 Ω) down to the required load impedance for optimum diode performance as an oscillator or amplifier. There are a number of ways of doing this; the two simplest techniques are the use of a (nominally) quarter-wave transformer, with characteristic impedance $Z_T < Z_o$ and the use of a shunt capacitor, C_L. These techniques are shown in Fig. 33, together with equations relating the parameters of the transforming elements to the resulting values of the load impedance presented to the diode. These elements principally determine the real part of the load impedance presented to the IMPATT diode, but also can have a strong effect on the load reactance. The *reactance* of the circuit, and hence the frequency of operation as an oscillator or the center frequency as an amplifier, can be controlled in several other ways; one is to *recess* the diode package into the ground plane as was done in the tunable cavity of Sec. IV.B. This lowers L_p, and raises the oscillation frequency. Another is to insert a section of line in the circuit between the diode and the frequency transforming element. This *raises* the circuit inductance and *lowers* the oscillation or center frequency. These methods are illustrated for a transformer-coupled circuit in Fig. 34. A third method is to vary

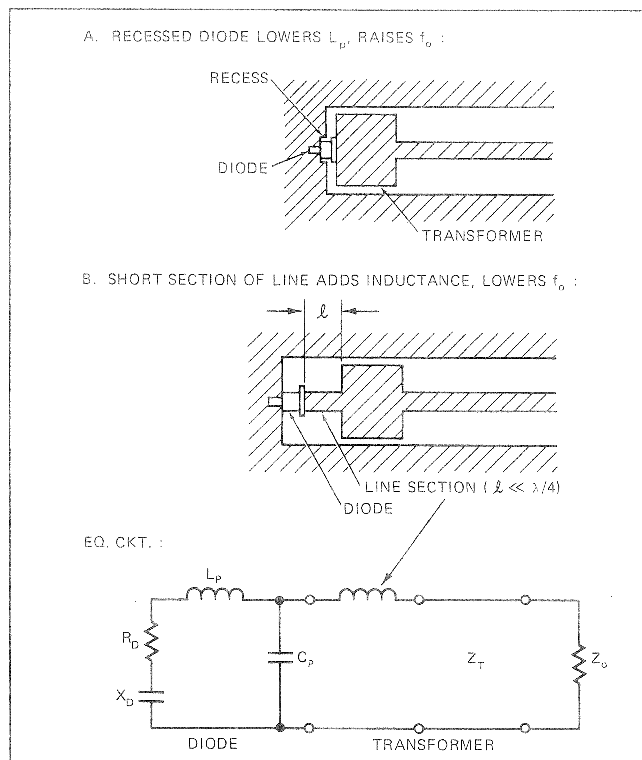

Fig. 34. Methods for Varying the Circuit Inductance in Low-Q Oscillators and Amplifiers.

SERIES EQUIVALENT CIRCUIT

$$R_L \simeq \frac{1}{(\omega C_L)^2 Z_O}$$

$$X_C \simeq \frac{1}{\omega C}$$

SERIES EQUIVALENT CIRCUIT FOR $\ell_T = \lambda/4$

$$R_L = \frac{Z_T^2}{Z_O}$$

Fig. 33. Basic Transformation Methods for Matching IMPATT Diodes in Low-Q Oscillators and Reflection Amplifiers.

the coaxial transmission line outer conductor diameter in the vicinity of the diode; this technique is used in the transformer-coupled cavity discussed in the next section. The coaxial oscillators and amplifiers described in this section require a bias T for operation.

A) *Oscillator Circuits*

Fig. 35 shows an oscillator circuit using a capacitor as the impedance-transforming element. The capacitor dielectric is composed of sheets of .001" Mylar, cut in the shape of washers; any dielectric with reasonable microwave properties can be used here. Fig. 36 shows output power and frequency plotted as functions of C_L for an HP 5082-0401 diode. The values of C_L were obtained by using different dielectric thicknesses, and were measured on a 1.0 MHz capacitance bridge. Capacitive reactance of C_L was measured at ~8 GHz on an HP automatic network analyzer; results were consistent within ± 10%. This type of circuit has been quite widely used at HP for evaluation of IMPATT diodes — its virtue is its extreme simplicity.

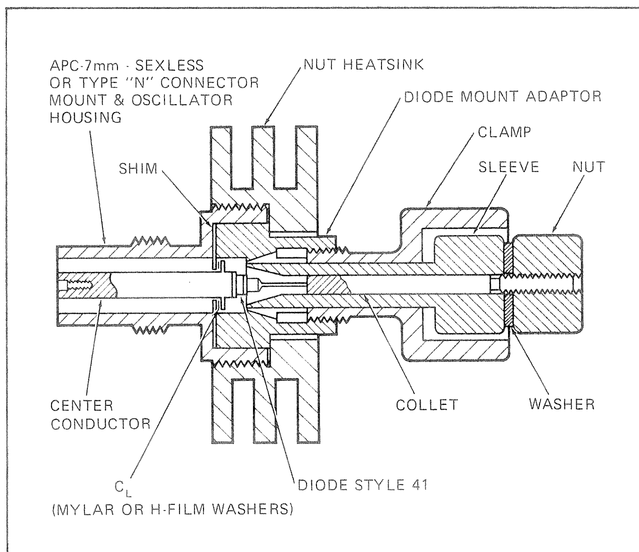

Fig. 35. An Oscillator Circuit Using a Capacitance as the Impedance Transforming Device.

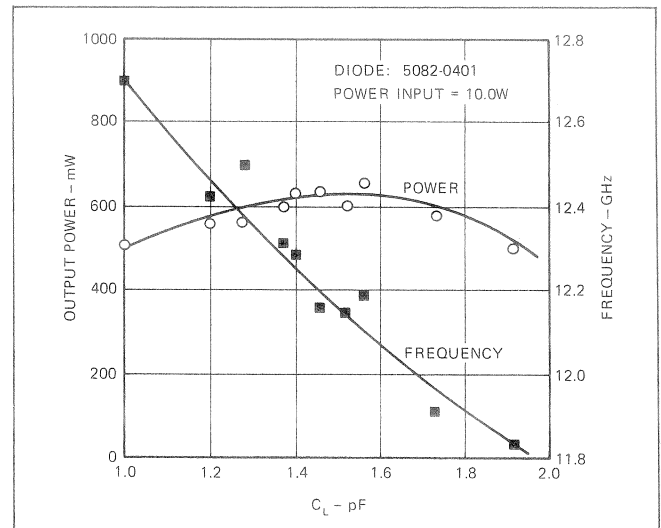

Fig. 36. Power and Frequency vs. C_L for the Circuit of Fig. 35 Using an HP-5082-0401 IMPATT Diode.

Fig. 37 shows a transformer-coupled oscillator circuit; Table III lists typical circuit dimension values for operation of HP 5082-0400/0401 IMPATT diodes at 8, 10 and 12 GHz. The output power obtainable from these diodes operated within their maximum ratings is between 0.5 and 0.8 W. The design of this oscillator is identical to that of the tunable oscillator shown in Fig. 23 — the only difference is that the spring loaded two-stage transformer is replaced by a single stage fixed transformer, and the tuning screw arrangement is replaced by the diode holder assembly of Fig. 10A. The injection phase-locking properties of this oscillator were investigated for a variety of injection signal powers with an output power of 550 mW and a free-running frequency, f_o, of 12.245 GHz, using an HP 5082-0401 diode. The results are plotted in Fig. 38 — these results are in good agreement with the simple locking theory of Adler[10, 11]; the appropriate equation is shown in the figure. The locking bandwidth, B_L, for known values of the injected signal power and the output power, can be used to calculate the effective circuit Q ("Q'_{ext}") using

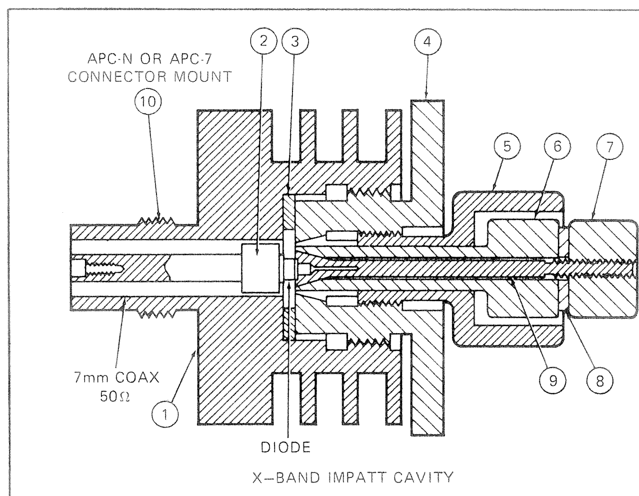

PARTS LIST			
ITEM	DESCRIPTION	MATERIAL	MANUFACTURER'S PART NO.
1	CAVITY BODY	BeCu (Alloy 172)	
2	TRANSFORMER	BRASS	
3	SPACER	BeCu (Alloy 172)	
4	NUT	"	
5	CLAMP	"	
6	SLEEVE	"	
7	NUT	STEEL	
8	WASHER		
9	COLLET	Berylco —10*	
10	CONNECTOR ASS'Y		AMPHENOL # 131-1050 (APC-7) # 131-10004 (APC-N)

*Beryllium Corporation, Distributor: E. Jordan Brooks, Inc., San Francisco

Fig. 37. A Laboratory Prototype Transformer-Coupled Oscillator. This Oscillator is the Basic Production Test Mount for HP IMPATT Diodes.

Adler's equation, and for this particular circuit a Q'_{ext} of about 18 is indicated.

The fact that a relatively high power IMPATT oscillator can be locked to a low-power highly stable source suggests its use in such applications as airborne Doppler navigation radar and radar altimeters. A typical low Q IMPATT oscillator using HP 5082-0400/0401 0.5 W IMPATT diodes, and fabricated from OFHC copper, has a temperature coefficient ranging from −40 ppm/°C at the low end of the specified operating frequency range of the diode to +20 ppm/°C at the upper end. At 10 GHz, these correspond to *total* variations of −60 MHz and +30 MHz, respectively, over the range −60°C to +80°C. Thus, over ambient temperature ranges commonly specified for military equipment, a 10 mW signal can easily keep a 500 mW oscillator in-injection locked.

B) *Amplifier Circuits*

As mentioned in the beginning of this section, an IMPATT diode can function as an *amplifier* if the load resistance presented to it is *larger* in magnitude than the

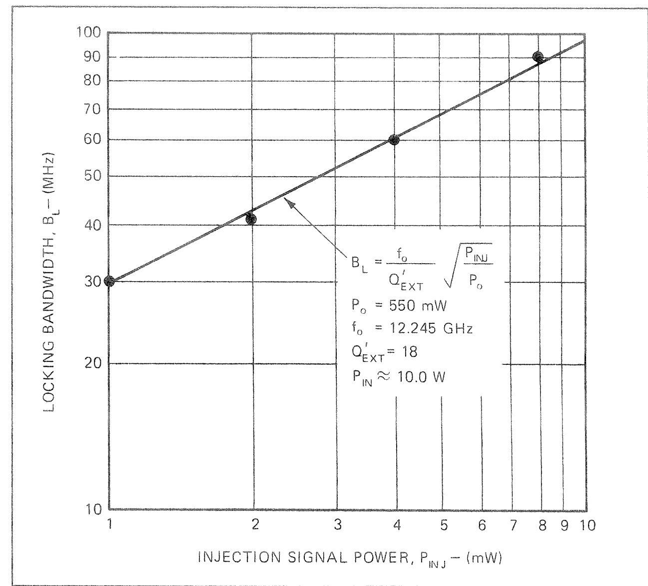

Fig. 38. Typical Injection-Locking Behavior of the Circuit Shown in Fig. 37. An Injected Signal of Only 10 mW is Sufficient to Lock the Oscillator Over a Range of ± 50 MHz in this Case.

TABLE III: Typical Transformer-Coupled Oscillator Dimensions for 8, 10, 12 GHz Operation

f_o (GHz)	TRANSFORMER LENGTH (inches)	TRANSFORMER DIAMETER (inches)	Z_T (Ω)	COLLET RECESS	SPACER INSIDE DIAMETER	SPACER THICKNESS (inches)
8	.15″	.245″	7.3	.01″	.610″	.048″
10	.15″	.245″	7.3	.01″	.280″	.048″
12	.15″	.235″	9.4	.035″	.220″	.020″

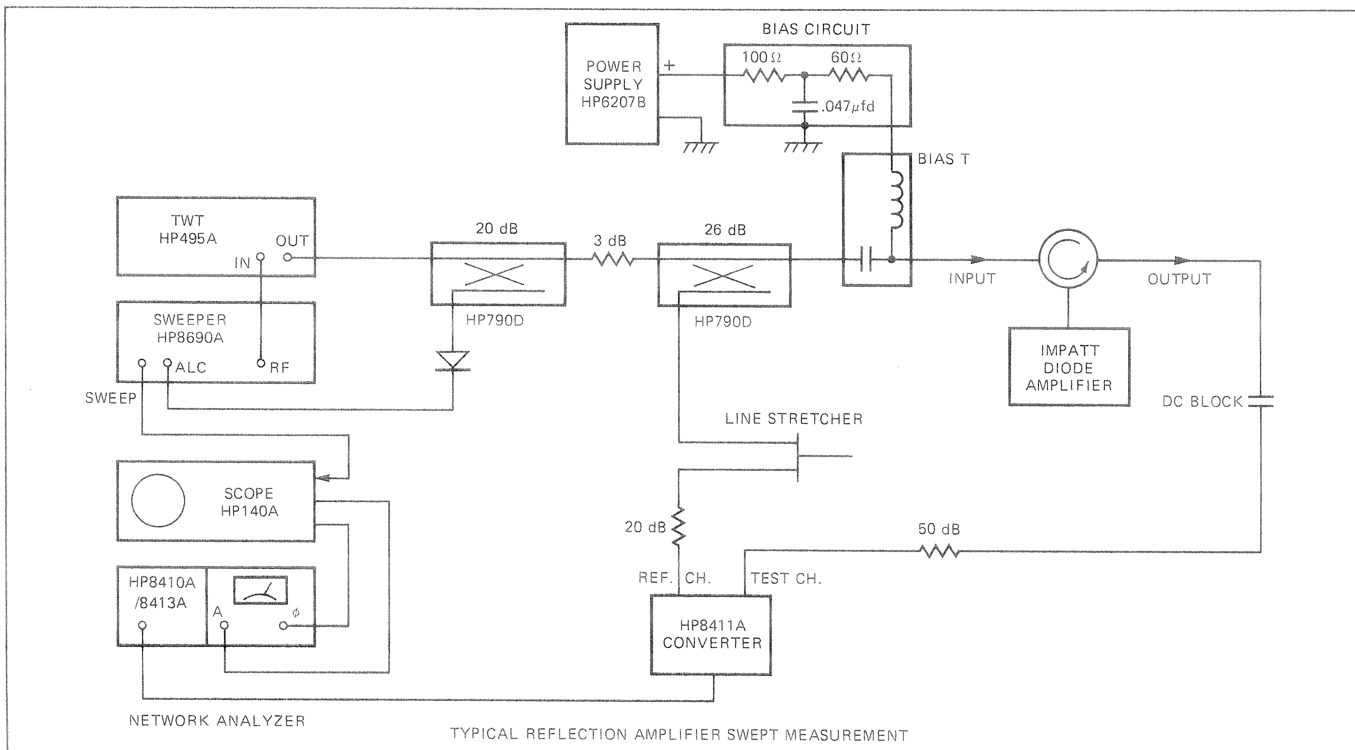

Fig. 39. Block Diagram of Reflection Amplifier Circuit.

diode's negative resistance, R_D. Both of the oscillator circuits illustrated in Part A of this section can be designed to operate as amplifiers with minor changes in C_L or the transformer characteristic impedance. In general, amplifier operation for a given diode requires a *smaller* value of C_L or a *larger* value for the transformer character impedance, Z_T, than for oscillator operation; both of these changes increase the value of the load resistance, R_L.

Fig. 39 shows the block diagram of a typical IMPATT reflection amplifier measurement circuit. A circulator is used to separate input and output signals. This circuit can measure the gain and phase shift of any amplifier or phase locked oscillator.

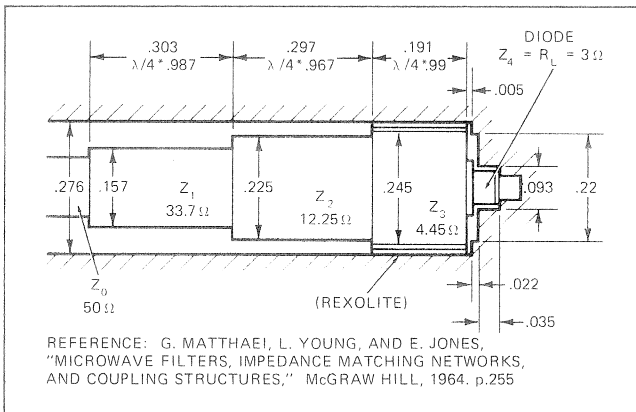

Fig. 40. Circuit Dimensions for an 11 GHz Amplifier.

Detailed circuit dimensions for an 11 GHz, 3-section transformer coupled amplifier are shown in Fig. 40. Three transformer sections provide somewhat greater bandwidth than a single quarter-wave transformer section. The center frequency for this amplifier is ~11 GHz, and the 3 dB bandwidth with 0.5 W output is ~1000 MHz. A gain of ~9 dB is obtained at the 0.5 W output level. Typical P_o vs. P_{IN} data are shown for various values of bias current in Fig. 41.

Measurements of reflection amplifier characteristics allow the determination of the R_D vs. I_D curve for a diode, such as we showed in Fig. 5. Typical data for an HP 5082-0401 diode at 11 GHz are shown in Fig. 42; several points have been verified by oscillator measurements as well, and are so indicated on the figure. The design procedure for an amplifier from the data of Figs. 41 and 42 is straightforward. First the center frequency, f_o, the frequency at which gain is maximum, must be selected. At this frequency, the circuit inductance (which may consist partly or entirely of the package inductance) resonates the junction reactance. The junction reactance can be estimated as the reactance of the junction capacitance at breakdown $C_j(V_b)$; typical values for $C_j(V_b)$ are listed in Table I in Section III. The data of Fig. 22C are useful in coaxial amplifier designs if a value of L_p less than about 0.6 nh is required. For higher values of circuit inductance, the technique of Fig. 34A can be used, or the outer conductor of the coaxial line at the diode can be enlarged as in Fig. 37.

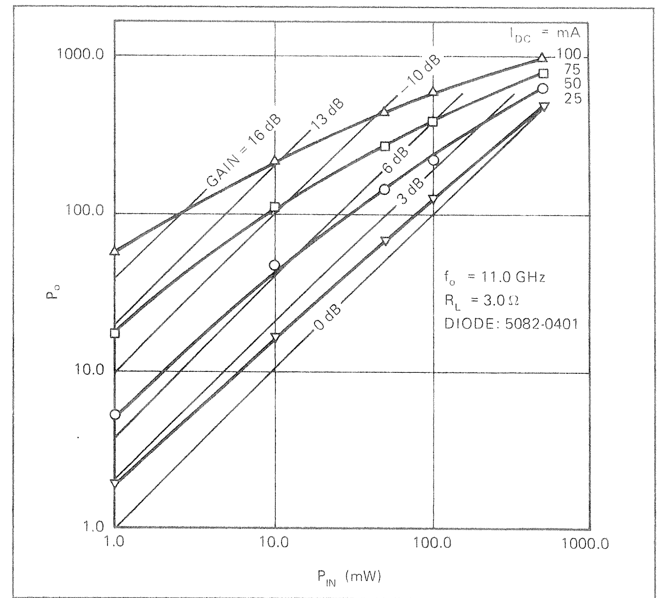

Fig. 41. P_o vs. P_{IN} for the Amplifier of Fig. 40 at Different Bias Currents.

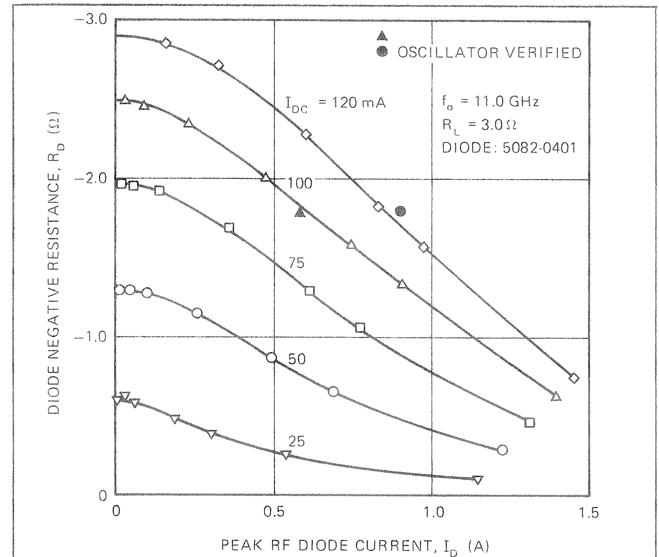

Fig. 42. Diode Negative Resistance, R_D, Plotted as a Function of the Diode RF Current Amplitude, I_D, for HP-5082-0401 Diode at 11 GHz.

Depending upon the exact circumstances, final adjustment of the circuit inductance necessary to achieve the desired center frequency is usually a cut-and-try process. At the center frequency, the power gain of the amplifier is given by

$$G_o = \left[\frac{R_D - R_L}{R_D + R_L}\right]^2 \qquad (12)$$

For example, if $R_D = -2\ \Omega$ and $R_L = 3\ \Omega$, the power gain is $[(-2\ -3)/(-2\ +3)]^2 = 25$, or 14 dB. An estimate for the power added by the amplifier is given by

$$P_A \approx \tfrac{1}{2} I_D^2 |R_D| \qquad (13)$$

For example, referring to Fig. 42, let us assume that $I_{DC} = 100$ mA, and that $R_D = -2\ \Omega$. The amplitude of the

diode RF current, I_D, is found as 0.50 A. Inserting these values in Eq. (14), we find $P_A \approx 0.250$ W; roughly, this is the maximum power we can expect from the amplifier at a gain of 14 dB. More power could be obtained, but at lower gain – for example at 1.2 Ω on the I_{DC} = 100 mA curve, we have $I_D \approx 1.0$ A and $P_A \approx 0.5$ W, but from (13), the gain is now about 7.5 dB.

The computations just given illustrate the methods used to obtain a preliminary design for an IMPATT amplifier; they also illustrate the fact that, since the IMPATT amplifier is non-linear, the gain is not independent of power level, but falls off with increasing power. The power levels achievable from a diode as an amplifier are about the same as the maximum power as an oscillator at the same frequency and the same DC bias current.

Fig. 43 illustrates a 9.0 GHz coaxial amplifier design, similar to the 11 GHz amplifier. Figs. 44 and 45 show P_o vs. P_{in} and R_D vs. I_D data, respectively, for an HP 5082-0400 diode.

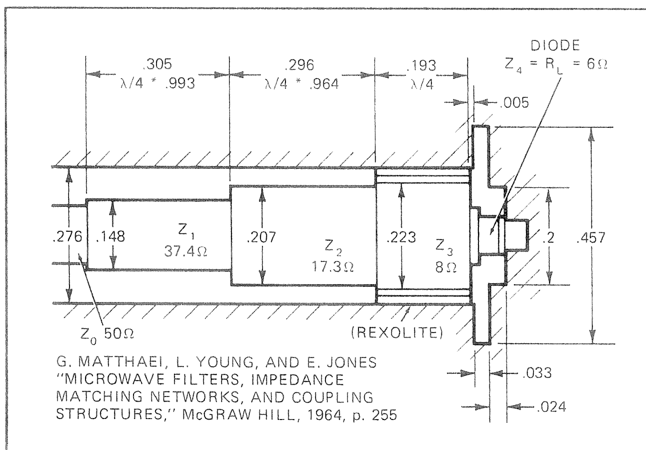

Fig. 43. A 9 GHz Coaxial Amplifier Design.

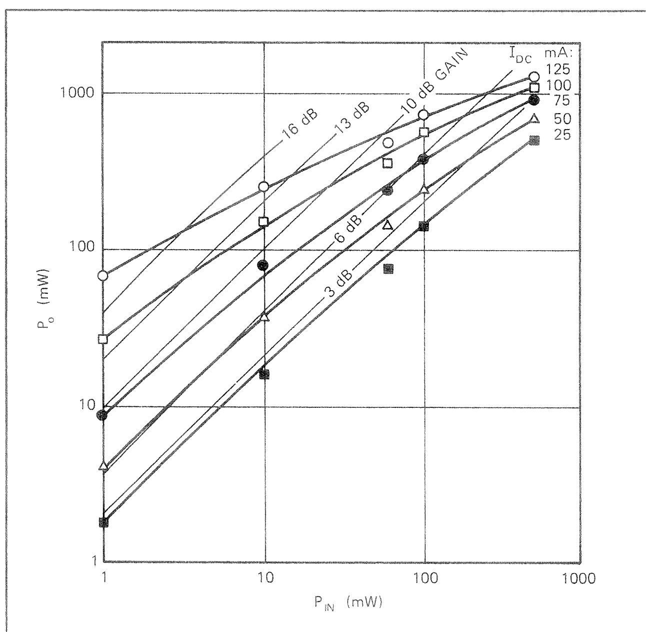

Fig. 44. P_o vs. P_{in} for the 9 GHz Amplifier.

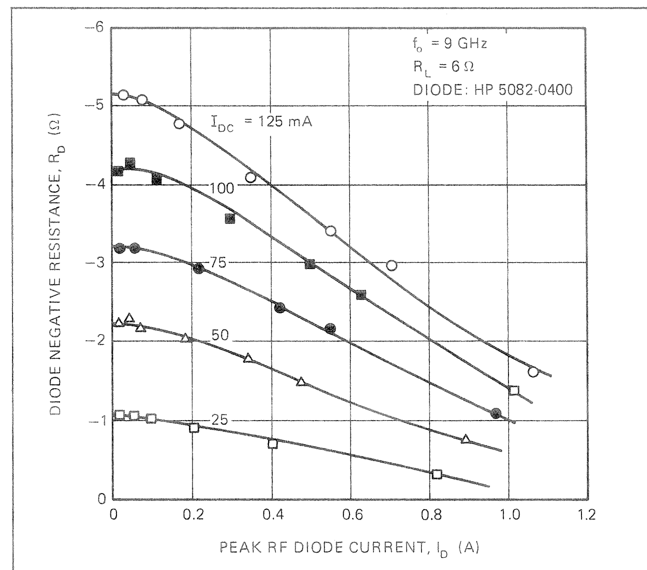

Fig. 45. R_D vs. I_D for an HP-5082-0400 Diode at 9 GHz.

Waveguide realizations of IMPATT amplifier circuits are also possible, but as of the time of preparing this Application Note, only limited information has been obtained on such circuits at Hewlett-Packard. The circuit of Fig. 46 illustrates a basic approach in waveguide amplifier design. Using a waveguide circulator to separate input and output signals, this circuit has produced more than 300 mW of output power at 12.4 GHz at a gain of about 8 dB. The DC input power was about 7.5 W, and the diode was an HP 5082-0400. The 3 dB bandwidth was about 200 MHz. Considerable further optimization of this circuit is possible, and more results on this and other waveguide amplifiers will be presented in a future Application Note.

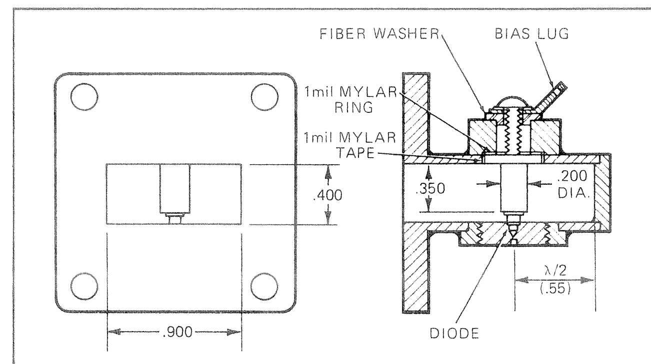

Fig. 46. Laboratory Prototype Waveguide IMPATT Amplifier.

It is often desirable to be able to estimate the diode RF current and voltage in an amplifier or oscillator. In order to make these estimates, the value of R_L presented to the diode must be known or estimated. Once R_L is known, the appropriate equations for obtaining V_D or I_D are:

$$V_D \approx \frac{\sqrt{2P_o\ R_L}}{\omega C_j(V_b)} \left[1 + \frac{1}{\sqrt{G_o}}\right] \qquad (14)$$

$$I_D \approx \omega C_j(V_b)\ V_D \qquad (15)$$

These are the peak values of RF voltage and current, respectively; G_o is the midband gain (infinite for an oscillator), and $C_j(V_b)$ is the junction capacitance at breakdown (Table I).

C) *Power Combining Techniques*

When power output requirements exceed the power obtainable from a single diode, methods for combining the power output of two or more oscillators (amplifiers), or two or more diodes in the same oscillator, must be considered.

Fig. 47 illustrates one method of combining the output power of two amplifiers. In this case, the amplifiers are simply connected in cascade, and the second stage is driven by the first with a signal large enough to reduce its gain to 3 dB. The two amplifiers then supply almost equal power to the load. The power levels shown in the example were taken directly from Fig. 41, assuming I_{DC} = 100 mA. The overall gain is 12 dB.

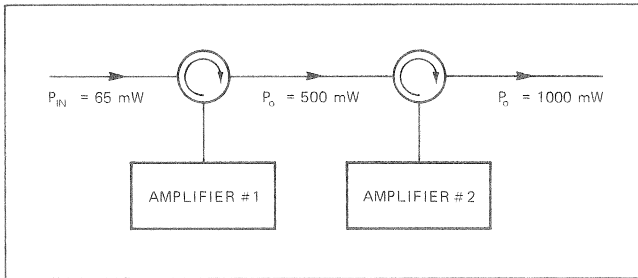

Fig. 47. Cascaded IMPATT Amplifiers.

A second technique for combining two amplifiers or oscillators is by the use of a 90° hybrid coupler as shown in Fig. 48. In the oscillator case this scheme allows an injection locking signal to be applied at the "input" port, or if no locking signal is used, this port is terminated in a matched load.

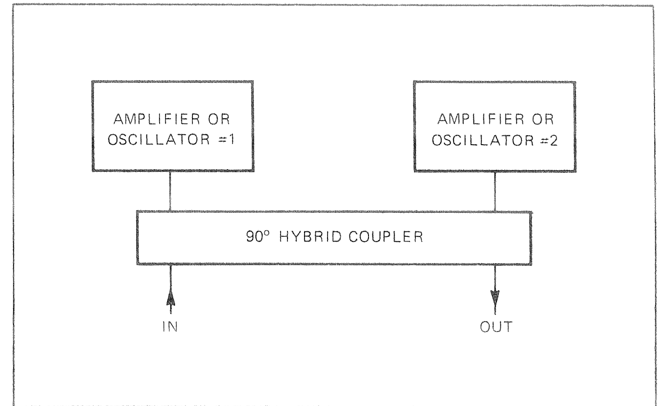

Fig. 48. Power Combining of Two Oscillators or Amplifiers Using a 90° Hybrid Coupler.

The reader is referred to references [12-20] for further reading on the subject of power combining of IMPATT diodes and oscillators. The works of Kurokawa and Magalhaes[15] and of Rucker[19] are particularly valuable contributions, which show the practical feasibility of obtaining CW output powers of 5 to 10 W from IMPATT oscillators in X-band.

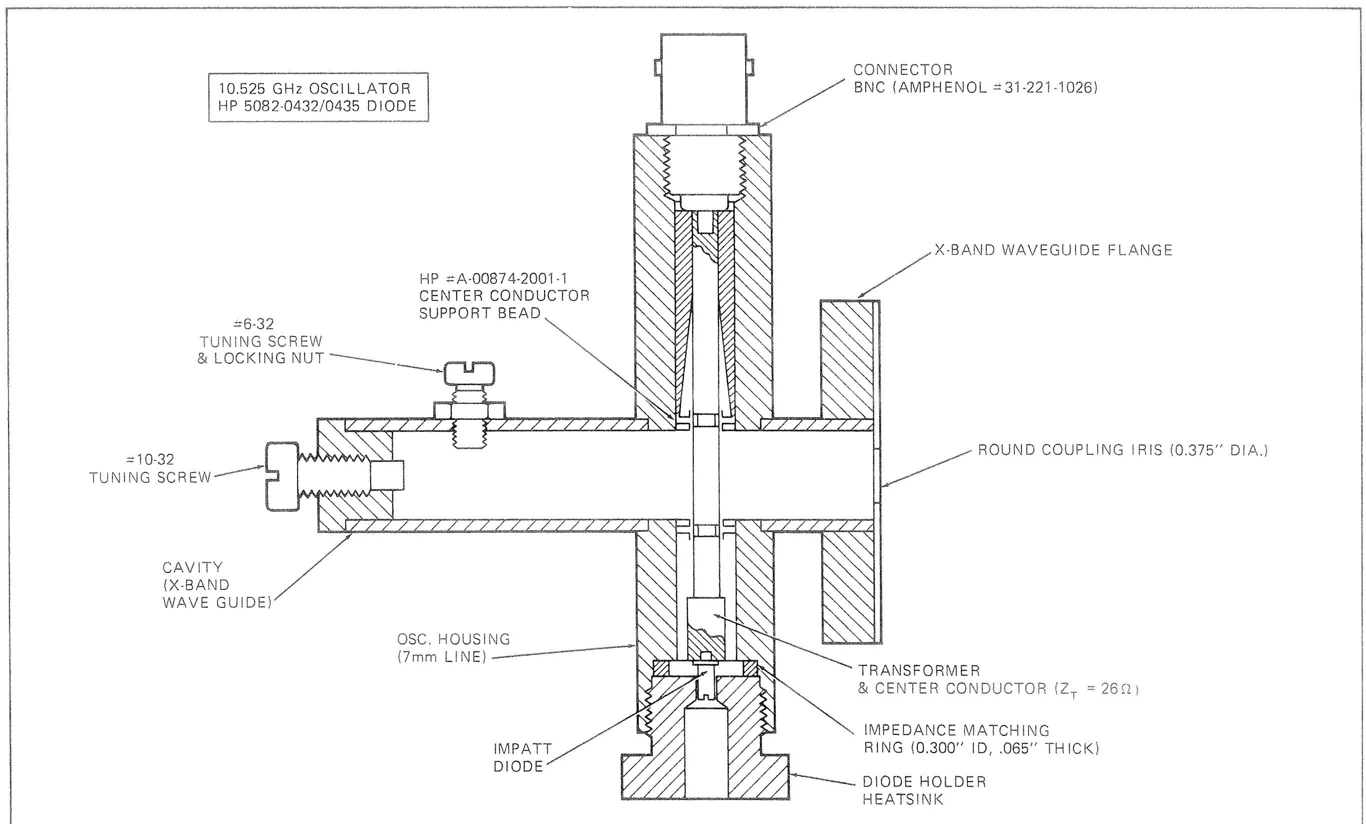

Fig. 49. Coupled Coax-Waveguide IMPATT Oscillator.

VI. High Q Low Noise Oscillators

Parts A and B of this section describe techniques for building high Q low noise IMPATT oscillators with essentially fixed tuning. The noise performance and frequency stability achievable with these oscillator designs is compatible with local oscillator requirements in radar, telemetry, and telecommunications receivers. Sufficient power is available from these oscillators to make them suitable for low power transmitters, and for parametric amplifier pumps, as well as police radars and intrusion alarms.

Part C describes typical results of experiment in which a commercial silicon microwave varactor diode is used to tune an IMPATT oscillator. This experiment shows that it is quite easy to achieve sufficient electronic tunability to employ AFC for the frequency stabilization of a high Q IMPATT oscillator, and to frequency-modulate it.

A) *Coupled Coaxial-Waveguide Oscillator*

The oscillator shown in Fig. 49 is a modification of a circuit design described by Magalhaes and Kurokawa[21] and by Kenyon[22]. The design basically consists of a coaxial oscillator which is strongly coupled to a high Q waveguide resonator. The waveguide resonator is in turn coupled by an iris to the load. Coupling between the coaxial circuit and the waveguide resonator is magnetic, and is obtained by passing the center conductor of the coaxial oscillator directly through the top (broad) wall of the resonator at a position corresponding to the magnetic field maximum in the resonator. The center conductor passes through a matched polyiron load to the bias connection. The best results in this oscillator have been achieved with the dimensions (in units of wavelength at the frequency of oscillation) shown in Fig. 50. The resonator is $3\lambda_g/2$ long, with the coaxial center conductor located approximately $\lambda_g/2$ from the iris, in the center of the waveguide. The length of the coaxial line from the guide center to the diode is fairly critical, and is close to $3\lambda/4$, including the $\lambda/4$ transformer. The function of the matched coaxial load is to prevent spurious resonances in the coaxial portion of the oscillator.

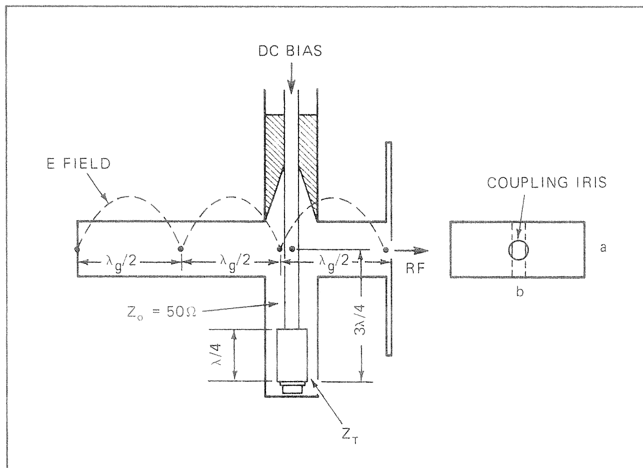

Fig. 50. Schematic Illustration of the Critical Dimensions in the Coupled Coax-Waveguide IMPATT Oscillator.

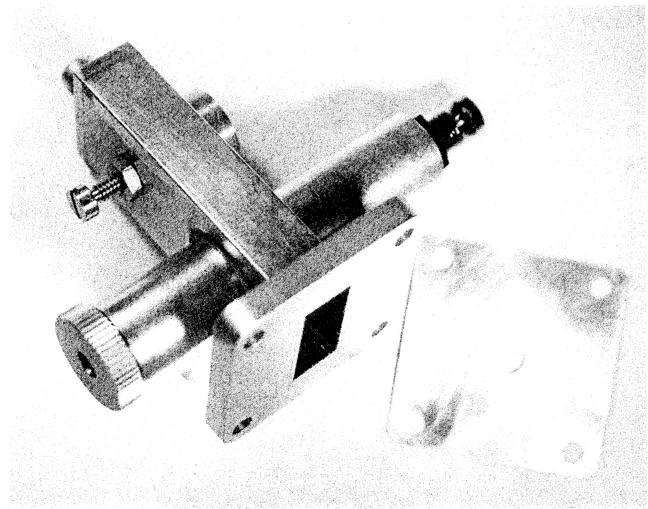

Fig. 51. Photograph of the Coupled Coax-Waveguide Oscillator.

It does not dissipate more than ~5% of the generated power in a properly designed oscillator.

A photograph of a laboratory model of this oscillator is shown in Fig. 51. This particular model was fabricated from brass. The parts are brazed together, using a stainless-steel mandrel to position and align the coaxial outer conductor parts. Accurate alignment of these parts is quite important for proper operation of this oscillator.

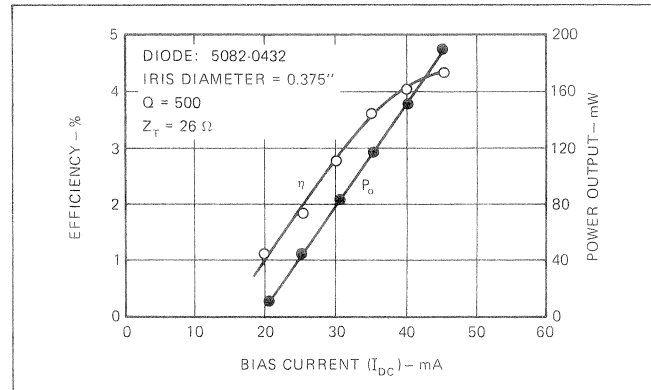

Fig. 52. Power and Efficiency vs. Bias Current for the Coupled Coax-Waveguide Oscillator of Fig. 49.

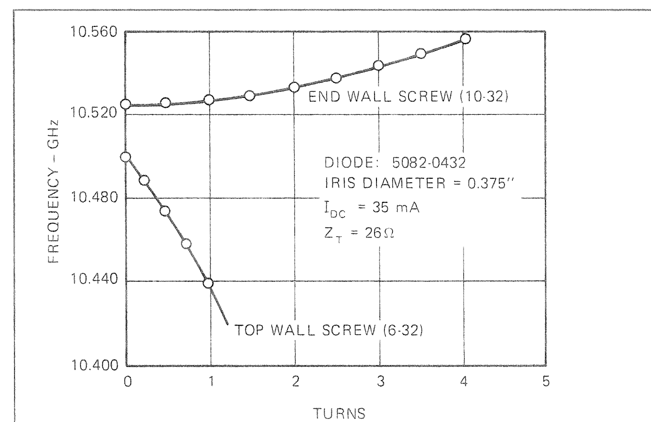

Fig. 53. Tuning Characteristics of the Oscillator of Fig. 49.

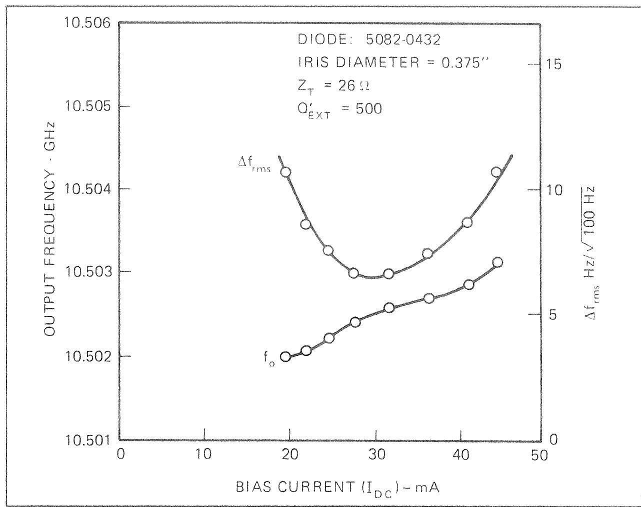

Fig. 54. Oscillation Frequency and FM Noise of the Oscillator of Fig. 49, as a Function of Bias Current.

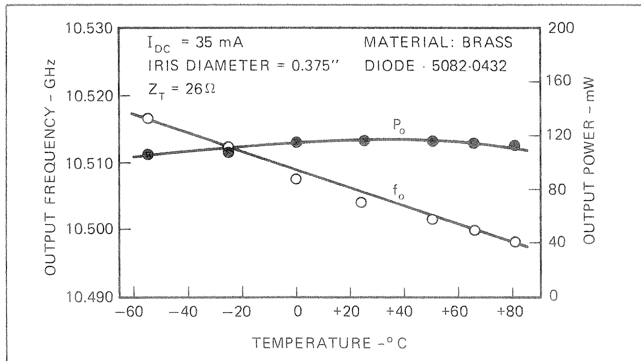

Fig. 55. Temperature Characteristics of the Oscillator of Fig. 49.

Typical results are shown in Figs. 52 through 55, for an oscillator with a Q of about 500. Figs. 56 and 57 show results for an oscillator in which the Q has been increased to about 2400. The increase in Q was obtained by reducing the iris diameter from 0.375" to 0.266". Increasing the Q has reduced the FM noise considerably, at the expense of a loss of output power.

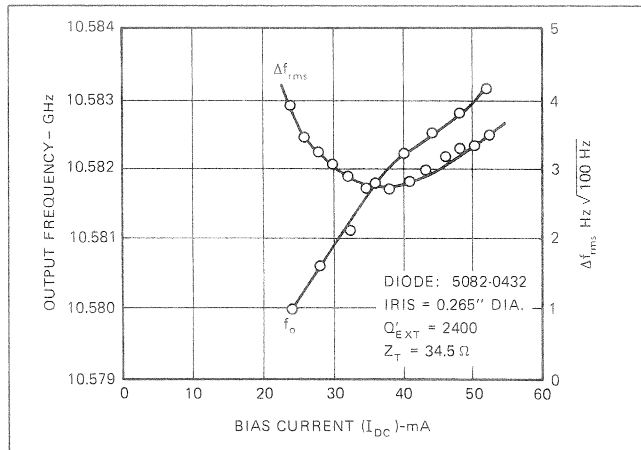

Fig. 56. FM Noise and Oscillation Frequency vs. Bias Current for a Higher Q (2400) Version of the Coupled Coax-Waveguide Oscillator.

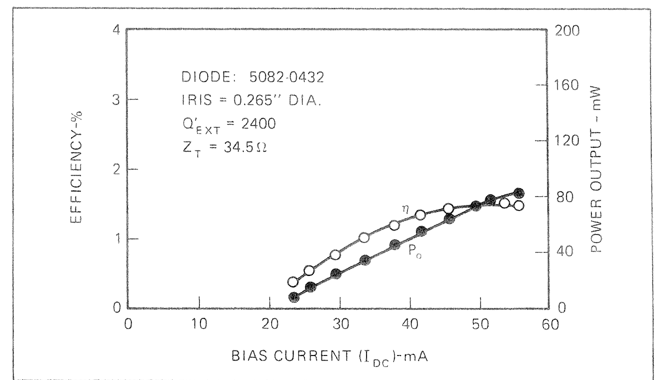

Fig. 57. Power and Efficiency vs. Bias Current for the Oscillator of Fig. 56.

The diodes used to obtain the results described above were HP 5082-0432 diodes. HP 5082-0401 diodes can also be used, with the following changes in dimensions: transformer impedance, 31 Ω; impedance matching ring, 0.144" ID x .055" thick; iris, 0.40" dia. Using these dimensions, more than 0.5 W can be achieved at ~5.0% efficiency with a typical 5082-0401 IMPATT diode. FM noise deviation is less than 10 Hz in a 100 Hz bandwidth, and the circuit Q is about 200. Typical data are shown in Fig. 58.

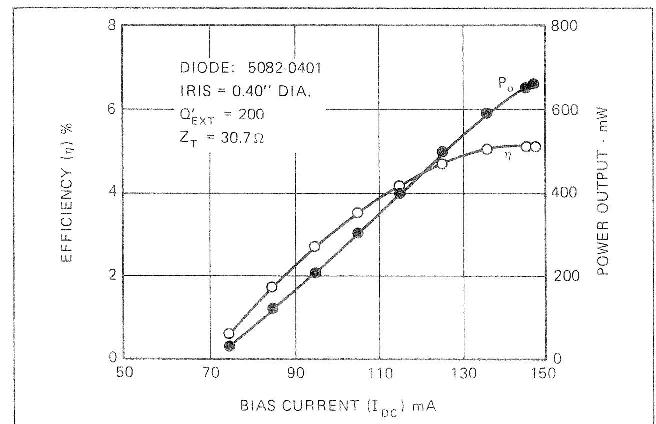

Fig. 58. Power and FM Noise vs. Bias Current for a 0.5 W Coupled Coax-Waveguide Oscillator.

The frequency-temperature behavior of the oscillator design shown here can be improved substantially by fabricating the waveguide resonator with Invar or stainless-steel and using an end plug of a material, e.g. brass, with a higher coefficient of expansion to compensate for length changes of the resonator. This concept is shown in Fig. 59. The basic idea is to select values for L_1 and L_2 which make the resonator length, L, remain approximately constant with temperature. It is quite easy to show that this requires

$$L_2 = \frac{1}{\frac{a_2}{a_1} - 1} L \tag{16}$$

where a_1 and a_2 are the temperature coefficients of expansion of the waveguide material and the plug, respectively. Obviously a_2 must be greater than a_1 for this concept

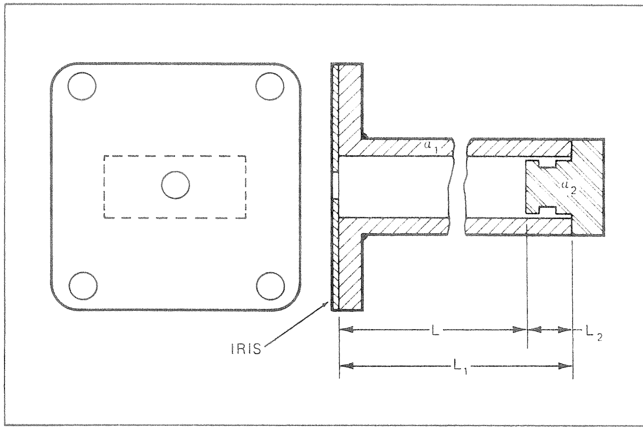

Fig. 59. Temperature Compensation Technique for the Coupled Coax-Waveguide Oscillator.

to work; the larger the ratio a_2/a_1, the shorter the temperature compensating plug can be. This technique has produced experimental oscillators similar to that of Fig. 49, with less than 1 ppm/°C variation of frequency with temperature, using Invar* waveguide with a brass plug.

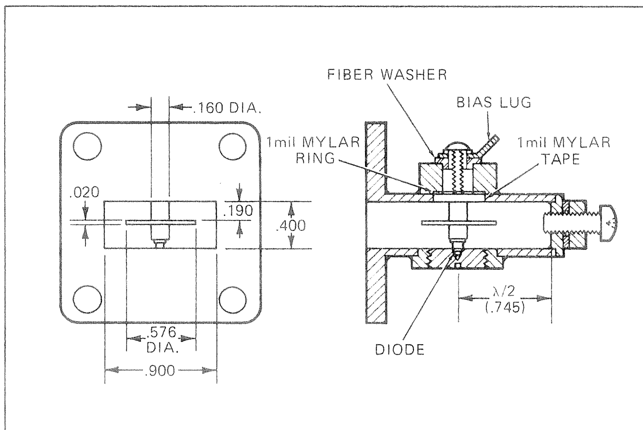

Fig. 60. Low Cost Waveguide Oscillator.

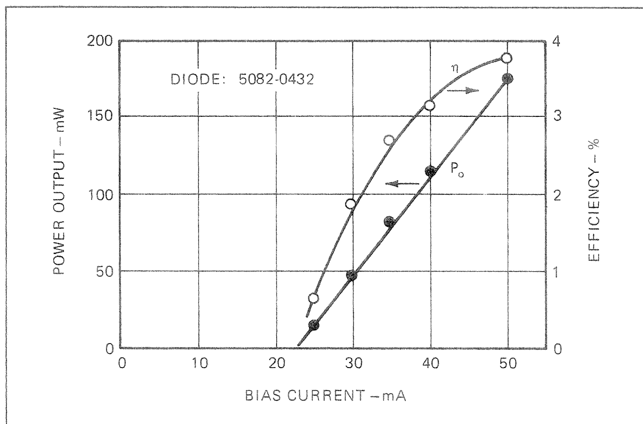

Fig. 61. Power and Efficiency of the Low Cost Waveguide Oscillator vs. Bias Current.

*WR90 Invar Waveguide is supplied by A. T. Wall Co., Van Nuys, California, and by Evered and Co. Metals Ltd. (represented by Connolly and Company, Inc., Mountain View, California).

B) *Low Cost Waveguide Oscillator*

The oscillator shown in Fig. 60 is essentially a modification of the oscillator of Fig. 28, incorporating a fixed short circuit. The configuration shown has a Q of about 1000, and was designed to operate at 10.6 GHz. Typical data are shown in Figs. 61 and 62. Fig. 62 shows a minimum in FM noise when plotted against I_{DC}; a similar effect was evident in Figs. 54 and 56. This behavior is predicted by a simple noise model discussed in Section VII. The temperature behavior of this oscillator is about the same as that of the oscillator shown in Fig. 28.

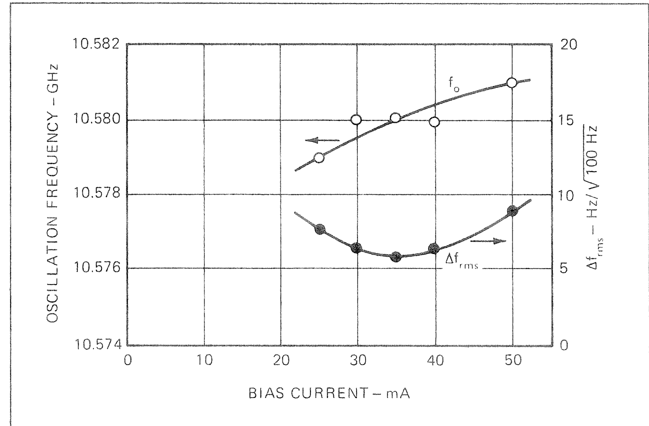

Fig. 62. FM Noise and Oscillation Frequency vs. Bias Current for the Low Cost Waveguide Oscillator.

This oscillator concept, because of its simplicity, is well-suited to applications where cost is an important factor, such as intrusion alarms, traffic control sensors, and, in general, any application requiring an inexpensive fixed-frequency microwave source. The design principles for this oscillator are less well known than for the oscillator discussed in the last section, which might make it somewhat more difficult to scale to other frequencies; general considerations for its design were discussed in Section IV.C.

C) *Varactor Tuning*

Some electronic tunability is usually required of an oscillator, either for frequency modulation or automatic frequency control. The oscillator of Fig. 49 has been varactor tuned over about ± 4.5 MHz without degradation of the oscillator FM noise, using a commercial silicon microwave tuning varactor in a special probe assembly*. The details are shown in Fig. 63, and the tuning data are shown in Fig. 64. The varactor probe has also been mounted inside the oscillator opposite the tuning screw in the broad wall of the waveguide resonator. The tuning range achievable without FM noise degradation was less in this case, about ± 1 MHz. The degree of coupling of the varactor to the oscillator is controlled in either case by the depth to which the probe is screwed into the waveguide wall. A locknut is used to tighten the probe when the desired depth is reached.

*This technique and the probe assembly design were suggested by R. Shipow of Spectra Electronics, Inc., Los Altos, California.

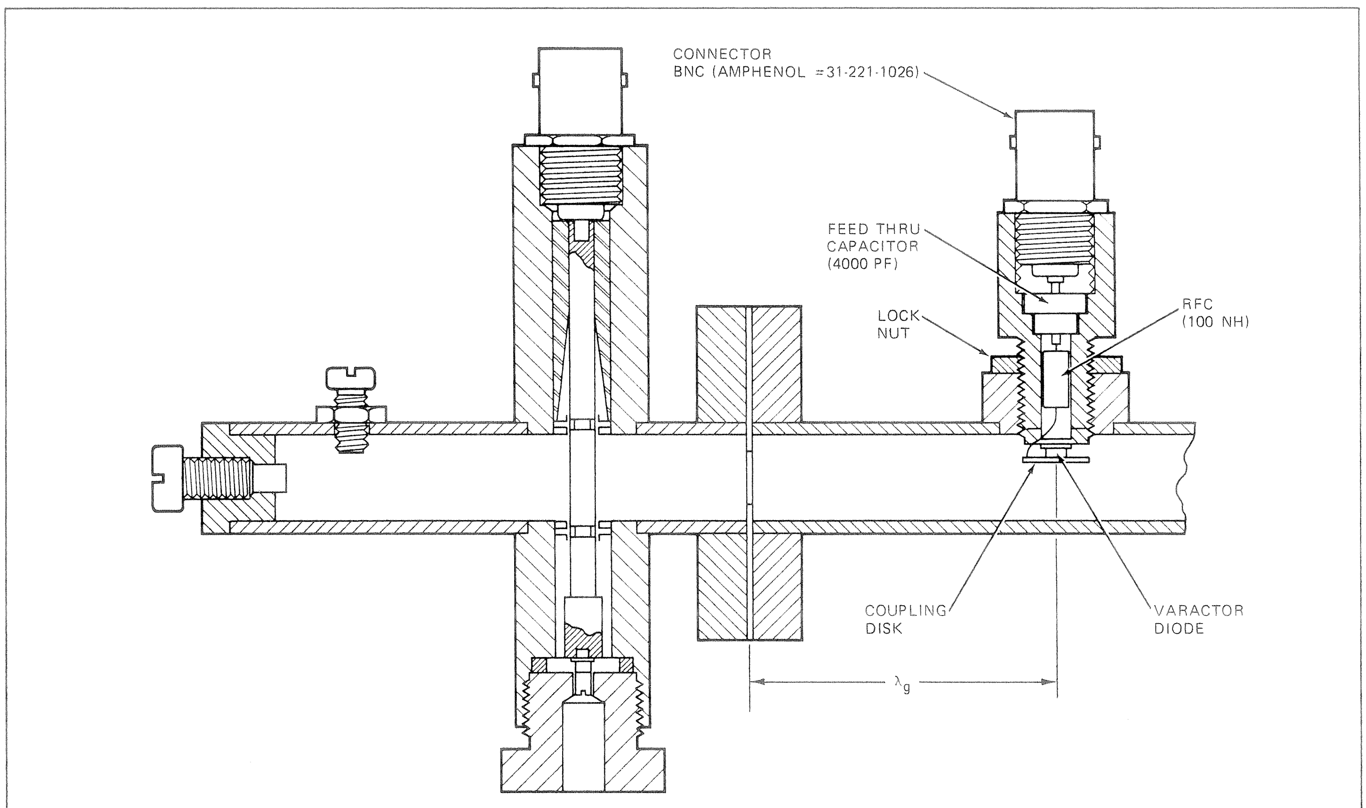

Fig. 63. Varactor Diode Mounting Technique for the Coupled Coax-Waveguide Oscillator.

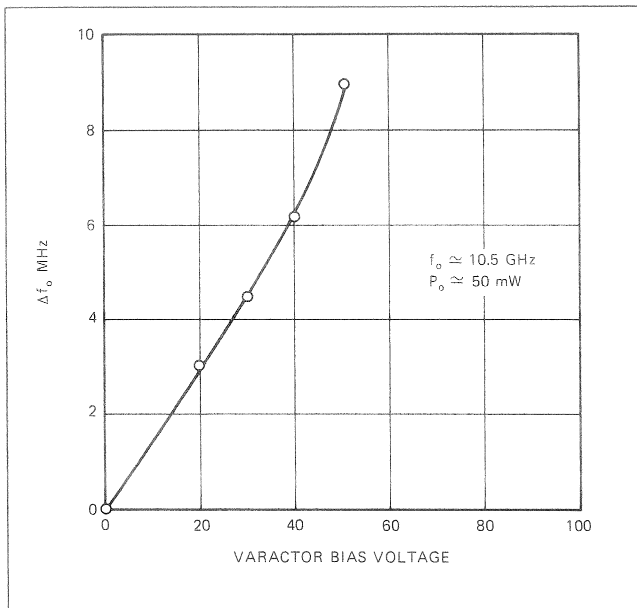

Fig. 64. Oscillation Frequency vs. Varactor Diode Bias Voltage for the Configuration Shown in Fig. 63.

VII. Noise in IMPATT Oscillators

When IMPATT devices first received consideration as practical microwave sources, there existed the rather widespread belief that these devices were too noisy to meet the stringent oscillator noise requirements of most military and commercial microwave systems. This belief has now been largely dispelled, but nevertheless, many prospective users of the devices wish to be able to compare the theoretically possible noise performance of IMPATT oscillators with other design alternatives, such as Gunn or reflex klystron oscillators. Part A of this section presents theoretical considerations which allow the noise performance of practical IMPATT oscillator designs to be predicted. In part B, typical IMPATT noise data are shown and are compared with data for typical Gunn and reflex klystron oscillators. Part C presents considerations for the proper operation of IMPATT devices in order to obtain the optimum noise performance, and discusses noise suppression techniques.

The general conclusion drawn from the theory and data presented in this section is that properly designed IMPATT oscillator circuits can have noise performance comparable to that of reflex klystron or Gunn oscillators in virtually *any* application. Of particular interest for systems with low intermediate frequencies (Doppler radars, for example) is the fact that HP IMPATT diodes exhibit no measurable "excess" or "1/f" noise near the carrier — this feature is not shared by Gunn and klystron oscillators, as will be seen in Part B. Freedom from 1/f noise means that the noise characteristics of IMPATT oscillators can be predicted quite accurately from basic oscillator noise theory, even very near the carrier. This facilitates oscillator design and allows system noise performance to be readily calculated.

A) *Noise Theory*

Noise behavior of oscillators is reasonably well understood now due to the early work of Edson[23], and more

recent contributions by Kurokawa [Ref. 11, p. 389] and Josenhans[24]. The theoretical expressions for FM and AM noise of any oscillator are given as follows:

$$\Delta f_{rms} = \frac{f_o}{Q'_{ext}} \sqrt{\frac{kT\ BM}{P_o}} \qquad (17)$$

$$\left(N/C\right)^{AM}_{SSB} = \frac{\frac{1}{2}\frac{kT\ BM}{P_o}}{\left(\frac{s}{2}\right)^2 + \left(\frac{Q_{ext}\ f_m}{f_o}\right)^2} \qquad (18)$$

where

- Δf_{rms} — The RMS noise deviation that would be measured in a bandwidth B at the output of an FM discriminator with the oscillator at its input.
- $\left(N/C\right)^{AM}_{SSB}$ — The single-sideband AM noise-to-carrier ratio in a bandwidth B measured at a distance f_m from the carrier.
- f_o — Oscillation frequency.
- P_o — Power output of the oscillator.
- B — Measurement bandwidth.
- k — Boltzmann constant.
- T — Ambient temperature.
- f_m — Distance from the carrier (commonly called the "modulation frequency").
- Q_{ext} — The true external Q of the oscillator.
- Q'_{ext} — The external Q as derived from injection phase locking measurements.
- s — A measure of diode nonlinearity. For maximum power output, s = 2.
- M — The Noise Measure of the oscillator.

The FM noise, expressed above as a noise deviation, can also be expressed as a noise-to-carrier ratio:

$$\left(\frac{N}{C}\right)^{FM}_{SSB} = \frac{\Delta f^2_{rms}}{2 f^2_m} \qquad (19)$$

The noise measure, M, sometimes called the noise temperature ratio, is a way of expressing the inherent noisiness of the active oscillator element relative to thermal noise, kTB. In a transistor or vacuum-tube feedback oscillator, the noise measure is simply the noise figure of the amplifier element. In klystron oscillators the noise is associated with fluctuations in the beam current. In solid state microwave oscillators such as IMPATT diodes and Gunn devices, the noise is associated with the inherent oscillation mechanism and in some cases with low-frequency fluctuation phenomena which amplitude and frequency-modulate the generated RF carrier.

The difference between the external Q as derived from locking bandwidth measurements (Fig. 38) and the "true" external Q arises from the nonlinear nature of oscillators, in particular the dependence of the active element's reactance on the AC current or voltage. Although not rigorously correct, it is usually an adequate engineering approximation to consider the two Q's to be equal. Also, the value of s in Eq. (18) can be taken to be 2 for most engineering purposes; then (18) becomes

$$\left(\frac{N}{C}\right)^{AM}_{SSB} = \frac{\frac{1}{2}\frac{kT\ BM}{P_o}}{1 + \left(\frac{Q_{ext}\ f_m}{f_o}\right)^2} \qquad (20)$$

The noise equations presented above are those derived from the assumption of "white" noise sources in the active oscillator element only. In practice, "excess" or "1/f" noise is also found to be important in some oscillators, especially in Gunn devices and klystrons; unfortunately, little is known theoretically about this kind of noise. Another important noise source in the case of IMPATT diodes is upconverted noise from the bias circuit. Proper bias circuit design, as discussed by Scherer[25] and described in Section III.D., eliminates this source of noise, so we will not discuss it here.

Equations (18) and (20), then, will form the basis for our discussion of silicon IMPATT diode noise. At the modulation frequencies for which noise close to the carrier is usually measured (f_m < 10 MHz) we expect Δf_{rms} and $(N/C)^{AM}_{SSB}$ to be *flat*, that is, not dependent on f_m. At a value of f_m given by

$$f_m \approx \frac{f_o}{Q_{EXT}} \qquad (21)$$

we should see the AM noise begin to fall off at the rate of 6 dB per octave. These features of the theory are observed to occur for HP IMPATT diodes; typical data is shown in the next section.

In order to compare the relative noise performance of IMPATT, Gunn and Klystron oscillators, we can tabulate measured values of M for the three devices. Actually, at least for IMPATT diodes, the behavior of M with signal level must be shown, too. The complete measured curve of M for typical HP silicon IMPATT diodes is shown in Fig. 65, plotted against the diode peak RF voltage normalized to the breakdown voltage. The minimum or "small signal" value of M is about 36 dB. This data was first published in [26], and has also been presented in somewhat different form in [27]. Reference [27] also shows data for GaAs IMPATT diodes, showing very similar behavior to silicon except that the minimum value of M is about 30 dB. The value of M for Gunn devices is extremely difficult to infer from published experimental data because of the presence of large amounts of 1/f noise. By considering only the data in the flat portion of the Δf_{rms} vs. f_m curve far from the carrier, values for M varying from roughly 25 to 35 dB are found for most Gunn oscillators. In many cases, the value of M for Gunn oscillators is academic because of the domin-

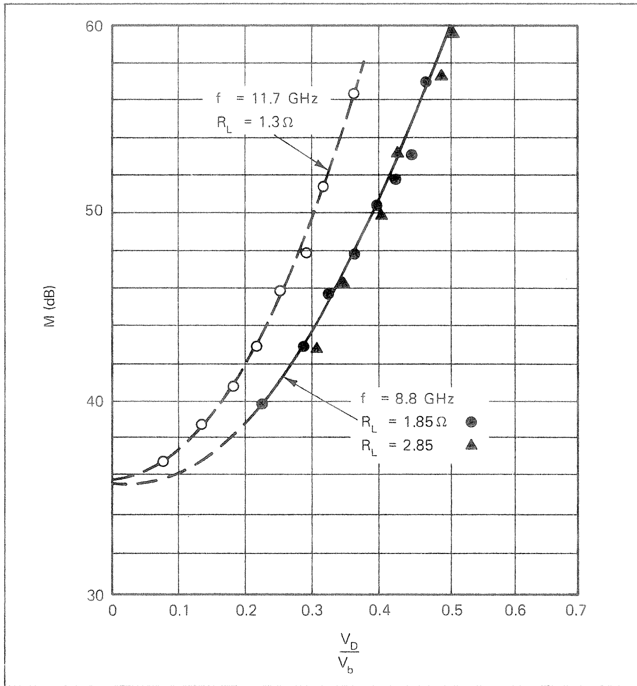

Fig. 65. Noise Measure of Typical HP (Silicon) IMPATT Diodes as a Function of the Peak RF Voltage Normalized to the Breakdown Voltage.

ance of 1/f noise near the carrier. Typical reflex klystrons will have values of M in the range of 40 to 45 dB; so-called low-noise klystrons have somewhat lower values, perhaps as low as 30 dB in some cases. Table IV lists the "small signal" M values for the various oscillator devices.

TABLE IV: Values of "Small Signal" M for Microwave Oscillator Devices

DEVICE	"SMALL SIGNAL" M (dB)
Silicon IMPATT	36
GaAs IMPATT	30
Gunn Device	25 – 35
Reflex Klystron	40 – 45
Low Noise Klystron	30 – 40

When Eq. (17) is used to predict FM noise for an IMPATT diode, it must be remembered that M is a function of RF voltage across the diode and therefore of power. In a fixed-tuned IMPATT circuit, as the microwave output power is increased by increasing the bias current, one sees at first a decrease in Δf_{rms}, since M is virtually constant at its "small signal" value, and Eq. (17) predicts that Δf_{rms} varies inversely with $\sqrt{P_o}$. At higher output powers, the dependence of M on RF level begins to overtake the inverse P_o dependence in Eq. (17), and Δf_{rms} will turn around and begin to increase. We thus expect a minimum in Δf_{rms} when it is plotted against either I_{DC} or P_o. This behavior is clearly seen in Figs. 54, 57 and 62. Similar considerations apply to AM noise.

A final remark on comparison of noise performance of oscillators is that, from (17) and (18) or (20), it is evident that, apart from the value of M, the noise depends on a number of parameters that are determined at least partially by the circuit in which the oscillator device is operated, namely the output power, the frequency and the external Q. Therefore, in order to compare the noise performance of different devices in different circuits, it is absolutely essential to know the values of P_o, f_o and Q_{EXT} for each circuit! This point is often overlooked in comparing noise performance, which has resulted in considerable confusion in the understanding of relative noise performance of microwave oscillators.

The next section presents curves of typical silicon IMPATT, Gunn and klystron oscillator noise data.

B) *Typical Data*

Fig. 66 is a plot of FM noise deviation (Δf_{rms}) vs. modulation frequency for typical X-band IMPATT, Gunn and klystron oscillators, all with power output in the range of about 100 mW. The IMPATT results were measured at Hewlett-Packard and by a commercial noise-measurement service*. The diodes used were HP 5082-0432 devices, and the circuit is that of Fig. 49. The specific data for the klystron are from Fig. 20 of [2]. The Gunn data are extrapolated from Fig. 16 of [28]. It is evident that both klystron and the Gunn device have considerable degradation in FM noise close to the carrier, due to "excess" or "1/f" noise. The data also indicate that excess noise is virtually absent in the two IMPATT oscillators shown. This has been found to be true in general for HP IMPATT diodes. An important point is that the high Q (Q_{EXT} = 2400) IMPATT oscillator has FM noise comparable to that of the klystron, and that its FM noise performance is quite adequate for FM telecommunication system local oscillators or upconverter pumps. Indeed, the performance and reliability of IMPATT oscillators as the carrier supply in long haul telephone repeater systems has been found superior to that of the conventional varactor multiplier chains presently used[29]. The advantage of the IMPATT is simplicity, leading to substantial cost savings over the multiplier chain approach.

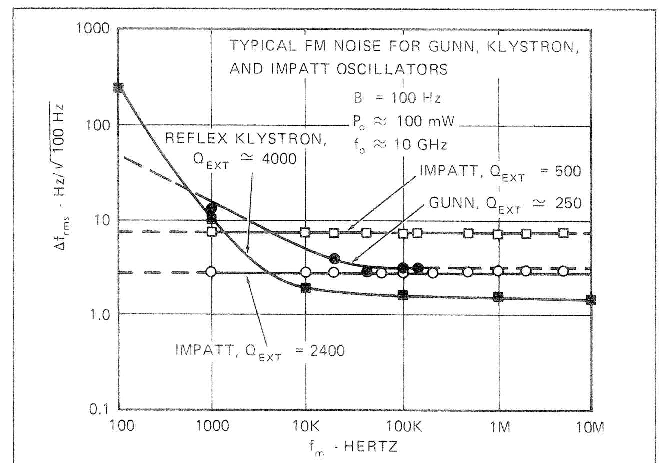

Fig. 66. FM Noise Performance of Typical X-Band Gunn, Reflex Klystron and IMPATT Oscillators with $P_o \simeq$ 100 mW.

*Spectra-Electronics, Inc., Los Altos, California

Fig. 67 shows the AM noise for typical IMPATT, Gunn and reflex klystron signal sources, again in a measurement bandwidth of 100 Hz and at a nominal power of 100 mW. The IMPATT and reflex klystron data were measured at Hewlett-Packard, and the Gunn data were taken from Fig. 15 of [28]. The klystron data can be compared to the data of Fig. 21 of [2] and are found to be very similar. Again, the klystron and Gunn oscillators show a substantial amount of excess noise. The apparent slight increase in the noise of the IMPATT oscillator below $f_m \simeq 2$ kHz is due to the excess noise of the detector element (a Schottky Barrier diode) used in the measurement system.

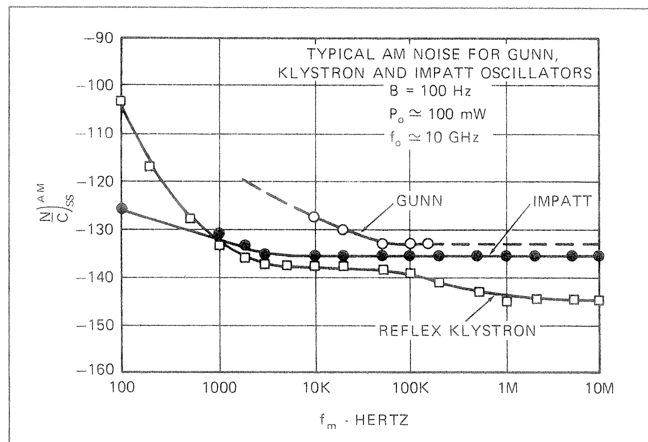

Fig. 67. AM Noise of Typical X-Band Gunn, Reflex Klystron and IMPATT Oscillators at 100 mW Output.

An important property of the AM noise in any high Q oscillator can be seen in Fig. 68. At the modulation frequency given by Eq. (21), as discussed, we expect the AM noise to have fallen to 3 dB from its "flat" value and to continue to fall at the rate of 6 dB per octave at higher f_m. A low frequency spectrum analyzer (HP 8553L) was used to make measurements on a high Q IMPATT oscillator out to f_m = 100 MHz, and the expected rolloff in AM noise was found; the −3 dB point calculated from (21) using the measured value of Q_{EXT} is in almost exact agreement with the measured −3 dB point, and occurs at $f_m \simeq 7$ MHz. The noise rolls off until the threshold of the measurement system is reached, corresponding to thermal noise (kT_oB) plus the system noise figure, F (13 dB in this case). The ramifications of this kind of behavior for AM receiver systems (e.g. radar) employing 30 or 60 MHz intermediate frequencies are quite clear: the IMPATT oscillator is capable of AM noise behavior comparable to that of a klystron local oscillator when operated in a moderately high Q circuit; if the Q is known, the achievable AM noise is given quite accurately by Eq. (20).

The FM noise measurements reported here were performed mainly with an HP 2590B Frequency Converter, which contains a 30 MHz discriminator, and with the IF preamplifier and demodulator sections of a commercial FM telecommunications receiver (Collins). Measurement threshold of the HP 2590B, about 2 Hz rms in a 100 Hz bandwidth, was somewhat better than that of the Collins re-

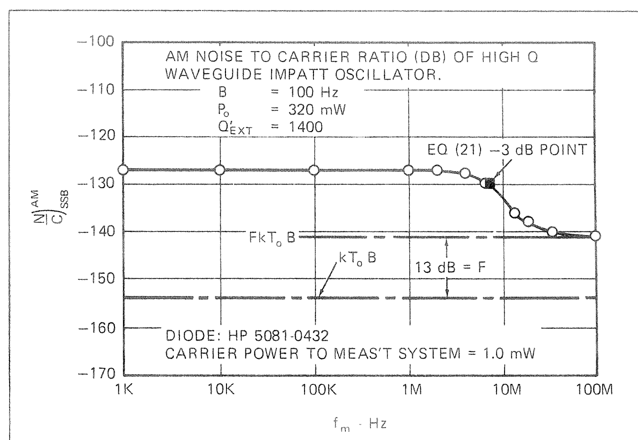

Fig. 68. AM Noise of a High Q IMPATT Oscillator Showing the Expected Reduction in Noise-to-Carrier Ratio at Higher Modulation Frequencies. The Calculated −3 dB Point, from Eq. (21), is Shown as the Black Square.

ceiver. The discriminator outputs of both systems are measured with a wave-analyzer. The measurement of the high Q IMPATT oscillator shown in Fig. 66 was performed by Spectra-Electronics, Inc., Los Altos, California, as a check on the other measurement methods. The AM noise measurements were performed using a high level detector in which the noise sidebands are down-converted to baseband by mixing with the carrier; the baseband signal is then amplified and measured with a wave-analyzer. The method is essentially that of Ashley, *et.al.*,[30], except that a single-ended detector was used in the present case.

C) *Noise Suppression*

From the RF circuit point of view, assuming that the bias circuit has been properly designed, the fundamental technique for obtaining optimum noise performance from an IMPATT oscillator is to operate the diode with the smallest value of RF voltage across the diode chip consistent with the required output power. This is obvious from Fig. 66, where we show the noise measure, M, plotted against the diode RF voltage normalized to the breakdown voltage. Fig. 66 could as well be a plot of M vs. I_D, the diode RF current, since diode current and voltage are related by Eq. (15). The crucial point is that if the RF voltage and current are allowed to be too high, M increases extremely rapidly, and the oscillator gets noisy.

For an oscillator with a fixed input power level, it is evident that the RF voltage and current are determined by the real part, R_L, of the load impedance presented to the diode chip, (Fig. 5). The choice of load resistance is therefore very important in IMPATT oscillator design. Fortunately, it is possible to achieve nearly the maximum output power in most IMPATT oscillators while obtaining the lowest noise. Fig. 69 shows this; here power and FM noise deviation are plotted against the real part of the load impedance, R_L. The higher values of R_L lead to lowest noise — this makes sense, since from Fig. 5 it is evident that higher values of R_L lead to *lower* values of I_D and hence *lower* values of V_D. The lowest Δf_{rms} is seen to be obtained at

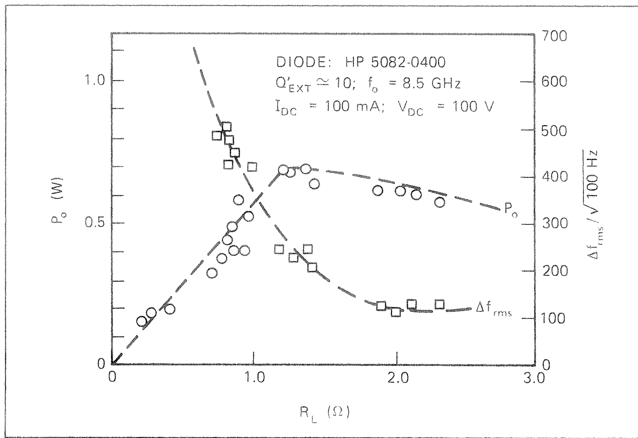

Fig. 69. Power Output and FM Noise of a Low Q Coaxial Oscillator as a Function of the Load Resistance, R_L.

the expense of only about 0.5 dB decrease in P_o from the maximum power. These data were taken in a low Q coaxial oscillator similar to that of Fig. 35. It is worth pointing out that the linear portion of P_o vs. R_L below $R_L \simeq 1.2\ \Omega$ corresponds to *saturation* in the IMPATT oscillator, in that at any R_L in this range, P_o does not increase with an increase in I_{DC}. This phenomenon occurs when the diode RF voltage reaches approximately ½ V_b. Operation in this range is extremely noisy, and usually leads to bias circuit instabilities such as were discussed in Section III.D. and III.E., especially if bias circuit design is not optimum. Operation in this range is avoided by providing a large enough value of R_L in the circuit*.

In most circuit designs, the achievement of the optimum value of R_L simultaneously with the circuit Q needed for low Δf_{rms} is done by cut-and-try. Some useful techniques were shown in Section VI. For high power and low noise, it is often easier to build a low Q oscillator such as those shown in Section V and to injection phase lock it with a lower power low noise source as in Fig. 70. Frequency stability can be achieved in this way at the same time. The degree of "quieting" which is possible by injection locking depends on many factors, which are conveniently summed up in the following equation:

$$\Delta f_{rms} = \sqrt{\frac{\Delta f_r^2 + \Delta f_{fro}^2 \cdot (f_m/B_L)^2}{1 + (f_m/B_L)^2}} \qquad (22)$$

The symbols in this equation have the following meaning:

- Δf_{rms} is the noise deviation of the injection locked IMPATT oscillator.
- Δf_{fro} is the noise deviation of the unlocked ("free running") IMPATT oscillator.
- Δf_r is the noise deviation of the low noise locking signal ("reference" signal).
- B_L is the locking bandwidth defined in Fig. 38.
- f_m is the modulation frequency.

The basic theory was developed by Hines, *et.al.,* [31]. The equation basically states that, near the carrier, the FM deviation of the locked oscillator is that of the reference signal, while far from the carrier it begins to take on the noise characteristics of the unlocked oscillator again. Injection phase locking has little effect on the AM noise spectrum.

From the preceding equation it can be shown easily for the usual case where $\Delta f_r \ll \Delta f_{fro}$ that the FM noise deviation of the locked oscillator has increased to $\sqrt{2}$ times Δf_r at a modulation frequency f'_m given by

$$f'_m \approx \frac{\Delta f_r}{\Delta f_{fro}} B_L \qquad (23)$$

As an example, take the oscillator from which Fig. 38 was obtained. It has a value of $\Delta f_{fro} \approx 70$ Hz in a 100 Hz bandwidth, independent of f_m. If the injected signal power is 10 mW, and Δf_r = 3.5 Hz, then the value of f'_m is about 5 MHz. To increase f'_m to 10 MHz, four times the injected signal power, or 40 mW, is needed. The expected form of the FM noise spectrum for these cases is shown in Fig. 71.

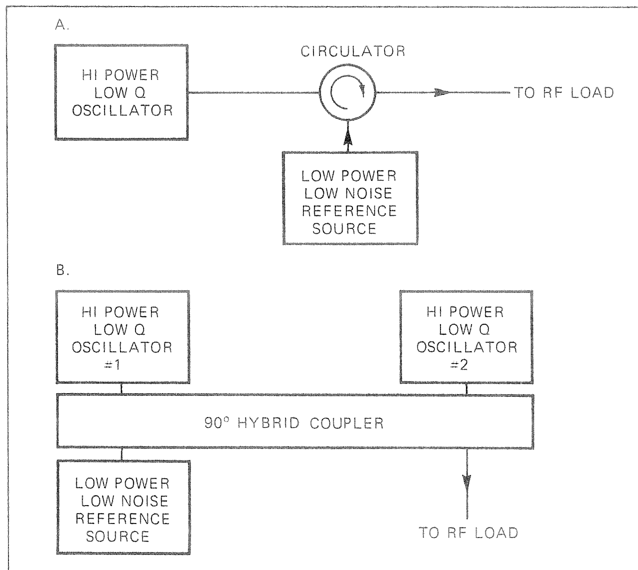

Fig. 70. Injection Phase Locking of One (A) and Two (B) Low Q IMPATT Oscillators with a Stable Low Noise Reference Source. The Arrangement in B Also Serves to Combine the Powers of the Two Oscillators.

*Equation (14) allows V_d to be determined from the values of P_o and R_L, if they are known.

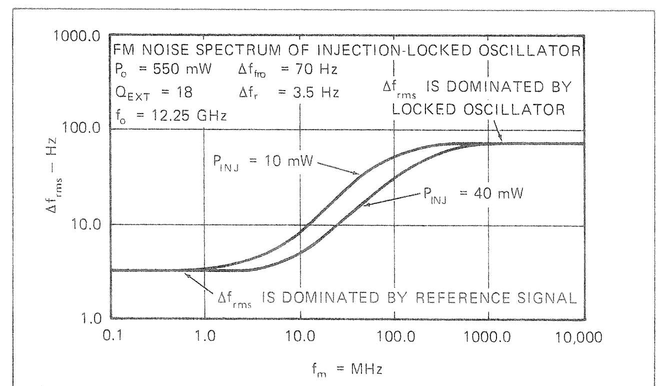

Fig. 71. FM Noise Spectrum of a 0.55 W Power Oscillator Injection Phase-Locked by a Quiet Low Power Reference Source.

APPENDIX A — IMPATT CIRCUIT DRAWINGS AVAILABLE FROM HP

Machine drawings for many of the circuits described in this Application Note are available as Hewlett Packard Publications, and can be ordered by HP Publication Number from the factory or from HP Field Sales offices. The available drawings are listed below.

Some of the circuits are designed for a specific HP IMPATT diode type. These circuits will work with other diode types with minor modifications in most cases.

IMPATT CIRCUIT DRAWINGS AVAILABLE FROM HP			
HP PUBLICATION NO.	DESCRIPTION	APPROX. FREQ.	SPECIFIC DESIGN FOR HP IMPATT TYPE NUMBER
5952-0261	Multiple-Slug Coaxial IMPATT Oscillator	5–16	All
5952-0262	Variable Inductance Coaxial IMPATT Oscillator	8–12	5082-0400 5082-0401
5952-0263	Tunable Waveguide IMPATT Oscillator	10.3–10.7	5082-0432 5082-0435 5082-0438
5952-0264	Low Q Coaxial IMPATT Oscillator (Transformer Coupled)	10 12.4 6.5 10.0 12.0	5082-0400 5082-0401 5082-0431/4/7 5082-0432/5/8 5082-0433/6/9
5952-0265	9 GHz Coaxial IMPATT Amplifier	$\sim$ 9.0	5082-0400
5952-0266	11 GHz Coaxial IMPATT Amplifier	$\sim$11.0	5082-0401
5952-0267	Coupled Coax-Waveguide IMPATT Oscillator (Waveguide Output)	10.5	5082-0401 5082-0432/5
5952-0268	Low Cost IMPATT Oscillator (Waveguide Output)	10.5	5082-0432/5
5952-0269	Coaxial Bias Tee	8.0–18.0	All

REFERENCES

[1] W. T. Read, Jr., "A Proposed High-Frequency Negative Resistance Diode", Bell Syst. Tech. J., 37, p. 401, (1958).

[2] G. I. Haddad, et.al., "Basic Principles and Properties of Avalanche Transit Time Devices". IEEE Trans. MTT, MTT-18, p. 752, (Nov. 1970).

[3] D. L. Scharfetter and H. K. Gummel, "Large-Signal Analysis of Silicon Read—Diode Oscillator", IEEE Trans. Electron Devices, ED-16, p. 64, (Jan. 1969).

[4] A. M. Cowley, "Design and Application of Silicon IMPATT Diodes", Hewlett-Packard J., 21, No. 9, p. 2, (May 1970).

[5] R. A. Zettler and A. M. Cowley, "Batch Fabrication of Integral Heat Sink IMPATT Diodes", Electronics Letters, 5, pp. 693-694, (27 December 1969).

[6] R. H. Haitz, et.al., "A Method For Heat Flow Resistance Measurements in Avalanche Diodes", IEEE Trans. Electron Devices, ED-16, p. 438, (May 1969).

[7] D. E. Iglesias, "Circuit for Testing High Efficiency IMPATT Diodes", Proc. IEEE, 55, p. 2065, (1967).

[8] G. L. Ragan, ed., "Microwave Transmission Circuits", Dover Publications, Inc., New York, pp. 466-472, (1965).

[9] "Reference Data For Radio Engineers", 4th ed., International Telephone and Telegraph Corporation, New York, p. 55, (1956).

[10] R. Adler, "A Study of Locking Phenomena in Oscillators", Proc. IRE, p. 351, (June 1946).

[11] K. Kurokawa, "An Introduction to the Theory of Microwave Circuits", Academic Press, New York, pp. 386-389, (1969).

[12] F. M. Magahaes and W. O. Schlosser, "A Series Connection of IMPATT Diodes", Proc. IEEE 56, p. 865, (May 1968).

[13] C. B. Swan, et.al., "Composite Avalanche Diode Structures for Increased Power Capability", IEEE Trans. Electron Devices, ED-14, p. 584, (Sept. 1967).

[14] F. Ivanek and V. G. K. Reddi, "Modular Approach to Higher-Power Avalanche-Diode Oscillators", Electronics Letters, 4, p. 446, (18 October 1968).

[15] K. Kurokawa and F. M. Magalhaes, "An X-band 10 Watt Multiple-IMPATT Oscillator", Proc. IEEE, 59, p. 102, (Jan. 1971).

[16] S. Mizushina, "2^N Oscillators Combined with 3 dB Directional Couplers for Output Power Summing", Proc. IEEE, 55, p. 2166, (Dec. 1967).

[17] W. O. Schlosser, A. L. Stillwell, "A Traveling-Wave Approach to the High-Power Solid State Oscillator", Proc. IEEE, 56, p. 1588, (Sept. 1968).

[18] H. Fukui, "Frequency Locking and Modulation of Microwave Silicon Avalanche Diode Oscillators", Proc. IEEE, 54, p. 1475, (Oct. 1966).

[19] C. T. Rucker, "A Multiple-Diode High-Average-Power Avalanche-Diode Oscillator", IEEE Trans. Microwave Theory and Techniques, MTT-17, p. 1156, (Dec. 1969).

[20] A. H. Solomon, et.al., "Microwave Generation from Avalanche Transit-Time Diodes", Final Report, U. S. Army Electronics Command Contract No. DAAB07-67-C-0671 (ARPA Order No. 692), (Dec. 1970).

[21] F. M. Magalhaes and K. Kurokawa, "A Single Tuned Oscillator for IMPATT Characterization", Proc. IEEE, 58, pp. 831-832, (May 1970).

[22] N. D. Kenyon, "A Circuit Design for MM-Wave IMPATT Oscillators", 1970 IEEE GMTT International Microwave Symposium Digest, pp. 300-303, (May 1970).

[23] W. A. Edson, "Noise in Oscillators", Proc. IRE, 48, p. 1454, (Aug. 1960).

[24] J. Josenhans, Unpublished work performed at Bell Telephone Laboratories.

[25] E. F. Scherer, "Investigations of the Noise Spectra of Avalanche Oscillators", IEEE Trans. Microwave Theory and Techniques, MTT-16, p. 781, (Sept. 1968).

[26] A. M. Cowley, et.al., "Noise and Power Saturation in Singly-Tuned IMPATT Oscillators", IEEE J. of Solid State Circuits, SC-5, p. 338, (Dec. 1970).

[27] J. Tatsuguchi, et.al., "Power-Noise Characterization of Phase-Locked IMPATT Oscillators", IEEE Int'l. Solid State Circuits Conference Digest, Phila. Penn., p. 170, (1971).

[28] S. Y. Narayan and F. Sterzer, "Transferred Electron Amplifiers and Oscillators", IEEE Trans. Microwave Theory and Techniques, MTT-18, p. 773, (Nov. 1970).

[29] "Electronics", p. 28, (1 March 1971). See also P. W. Nield, "An IMPATT Generator for 6 GHz Long-Haul Radio", IEEE ISSCC Digest, p. 224, (Feb. 1971).

[30] J. R. Ashley, et.al., "The Measurement of Oscillator Noise at Microwave Frequencies", IEEE Trans. Microwave Theory and Techniques, MTT-16, p. 753, (Sept. 1968).

[31] M. E. Hines, et.al., "FM Noise Suppression of an Injection Phase-Locked Oscillator", IEEE Trans. Microwave Theory and Techniques, MTT-16, p. 738, (Sept. 1968).

For more information, call your local HP Sales Office or East (201) 265-5000 • Midwest (312) 677-0400 • South (404) 436-6181 West (213) 877-1282. Or, write: Hewlett-Packard, 1501 Page Mill Road, Palo Alto, California 94304. In Europe, 1217 Meyrin-Geneva

COMPONENTS

Printed in U.S.A.

5952-0260(6/71)